AN ANALYSIS OF TRANSIENT HEAT FLOW THROUGH A COMPOSITE WALL

by

JAMES W. McDONALD

B.A.Sc., University of British Columbia, 1958

A THESIS SUBMITTED IN PARTIAL FULFILMENT OF

THE REQUIREMENTS FOR THE DEGREE OF

MASTER OF APPLIED SCIENCE

in the Department

of

MECHANICAL ENGINEERING

We accept this thesis as conforming to the
required standard

THE UNIVERSITY OF BRITISH COLUMBIA

April, 1962

In presenting this thesis in partial fulfilment of the requirements for an advanced degree at the University of British Columbia, I agree that the Library shall make it freely available for reference and study. I further agree that permission for extensive copying of this thesis for scholarly purposes may be granted by the Head of my Department or by his representatives. It is understood that copying or publication of this thesis for financial gain shall not be allowed without my written permission.

Department of Mechanical Engineering

The University of British Columbia,
Vancouver 8, Canada.

Date April 24, 1962

ABSTRACT

The object of this investigation was to examine the transient heat flow through a composite wall. This wall was chosen to represent the type used in house construction. It consisted of a fir frame, covered on one side with hardboard and on the other with cedar, and the space between the hardboard and cedar was filled with fibreglass insulation. A vapour barrier was not included as it would offer little resistance to heat flow. This structure, therefore, offered resistances to heat flow in series and parallel.

The theoretical analysis was numerical owing to the anisotropic properties of the materials and to the composite structure of the wall. Two analyses were made of the transient heat flow, an exact analysis and an approximate analysis which neglected the effect of the frame. The heat flow was three dimensional in the first analysis owing to the difference in the magnitude of the parallel resistances and was one dimensional in the approximate analysis. The two theoretical solutions both showed exponential cooling rates and agreed within five percent of each other, which shows that the effect of the frame is negligible when its surface area is small as compared to the total surface area of the wall. The ratio of total wall surface area to frame area for the wall studied was 9.6 to 1.0.

The wall was mounted in a guarded hot-box apparatus and experiments were performed in order to verify the results of the theoretical analysis. The experiments consisted of establishing

a steady state temperature gradient across the wall and then eliminating the heat source. The ensuing transient temperatures were measured by thermocouples and were compared with those predicted by theory. The experimental results varied from the exact solution by 14 percent and from the approximate solution by 18 percent. The experimental results indicated that the tests were consistent.

The difference between the theoretical and experimental results was attributed to: (1) contact resistances, (2) nonhomogeneous wall materials, (3) nonuniform surface coefficients of heat transfer, and (4) the effect of neglecting certain heat capacities which actually were not negligible.

The results indicated that the transient temperatures varied according to the equation $T = Ti\ e^{-\frac{t}{\tau}}$ where T represents temperature, t represents time, and τ is the time constant. The results also showed that the method of analysis was acceptable and that the approximate analysis is suitable for walls with small frame areas.

ACKNOWLEDGMENT

The writer wishes to express his gratitude to Professors W. A. Wolfe and J. L. Wighton for their supervision of the thesis, to W. Hancock of The British Columbia Forest Products Laboratory for his assistance, to W. O. Richmond, and the entire Department of Mechanical Engineering, University of British Columbia.

This research was made possible by funds supplied by the National Research Council, under a grant to Professor W. O. Richmond.

TABLE OF CONTENTS

INTRODUCTION

A study was started ten years ago in the Department of Mechanical Engineering at the University of British Columbia of the heat transfer conditions involved in the transient heating of buildings and houses. The initial phase was the investigation of the transient response of heated air in an enclosure with heat losses through a concrete slab. Experiments were performed under the direction of Mr. G. Green, on the air enclosure and slab in a guarded hot-box apparatus using step and cyclic changes in the heat supply. A paper covering the analytic investigation was written by Professor W. A. Wolfe and published in 1959.[1] This paper, which considered the heat capacity of the fluid in the enclosure, predicted the transient temperatures of the air enclosure and the inside surface of the slab. This was a refinement on a previous paper by E. G. Smith which did not consider the heat capacity of the enclosed fluid.[2] The results of the paper by W. A. Wolfe showed that when the fluid is air, the heat capacity can be neglected. In the discussion of his paper, it was suggested that this type of problem could be solved numerically if a multilayer wall were available. Thus, from this suggestion, it was decided to investigate the heat transfer properties of a frame wall typical of house construction.

---

1. W. A. Wolfe, "Transient Response of Heated Air in an Enclosure With Heat Losses", Journal of Heat Transfer, 81: 19-23, February, 1959.

2. E. G. Smith, "A Simple and Rigorous Method for the Determination of Heat Requirements of Simple Intermittently Heated Exterior Walls", Journal of Applied Physics, 12:638-642, 1941.

DESCRIPTION OF THE APPARATUS

The apparatus, shown in Figures 2 and 3, consisted of four principle parts: (1) the wall, (2) the test section, (3) the guard section, and (4) the exit section.

The Wall

The wall consisted of a fir frame, covered on one side with hardboard, and on the other with a cedar panel. The studs were spaced on centres 16 inches apart, and the girts were spaced on centres 28 inches apart, in the section of the frame in the region of the test section (Figures 4 and 5). The components of the frame were carefully fitted together in order to reduce contact resistances. The components of the frame were selected with a straight grain, in order that the heat flow would be either normal to or parallel with the grain. This is important as the grain causes anisotropy in wood.[3]

Hardboard was glued and tightly screwed to the hot side of the frame in an effort to reduce contact resistances produced by air spaces. A cedar panel was securely fastened to the cold side of the frame. Access to the interior of the wall was facilitated by constructing the cedar panel in such a manner that it could be

3. Appendix B.

removed intact. With this arrangement, insulation could be changed, and thermocouples relocated.

A fibreglass insulation was installed for the experiments performed in this study, and was compressed into place to ensure a good thermal contact with the fir, hardboard and cedar. Due to the anisotropic properties of wood, edge cut cedar with a straight grain was selected for the cedar panel. The panel was also constructed to minimize the effects of air spaces between the boards.

The Test Section

The temperature measurements were taken in the test section, which was the centre portion of the wall, plus an adjacent air enclosure (Figures 2 and 5). The sides of the test section were away from the edge of the wall in order that the heat losses at the edges would not affect the temperatures in the test section. A control system prevented any transfer of heat across the boundaries of the air enclosure. Thus, all the heat in the test section passed directly through the wall.

The casing of the test section consisted of aluminum coated heavy kraft paper, insulated by an aluminum lined fibreglass insulation, with the lining on the outside to prevent radiation to the test section. This insulation was used to decrease the response of the test section to the surrounding guard section.

Two heaters, one of four ohms resistance, and the other of six ohms, were suspended in the test section. They could be used

separately, together, in parallel, or series, depending on the power required. The voltage to the heaters was controlled by a variac, and this voltage determined the temperature difference across the wall. These heaters had radiation shields in order to prevent radiation to the wall, since only conduction heat transfer was desired.

A balsa wood fan was placed in the test section to mix the air, and create a uniform surface coefficient over the surface of the wall. This fan was driven by an electric motor, which was on the outside of the apparatus.

The Guard Section

The function of the guard section was to isolate the test section. It surrounded the test section, and was enclosed by a plywood casing, with two plastic windows for viewing the inside of the apparatus (Figures 1, 2, and 3). This casing was lined with fibreglass insulation in order to reduce heat losses.

Ribbon heaters, supported by wooden rods with porcelain insulators, encircled the test section to give a uniform heat generation throughout the guard section. There were ten of these heaters in the guard section which could be used on a continuous 110 volts, and five that were connected to the output of the variac in the control system. This arrangement gave a better temperature control than that given by connecting all the heaters to the variac.

Two fans, mounted in opposite corners of the apparatus, circulated the air and produced a uniform temperature throughout the guard section. Aluminum coated paper was attached to wire supports to form a radiation barrier between the ribbon heaters and the test section. This barrier directed the air to encircle the test section.

The Exit Section

The exit section was an air enclosure on the cold side of the wall, formed by covering a steel frame with aluminum coated paper. The aluminum covering opposite the wall was coated with brown paper, in order to prevent radiation from the heaters being reflected to the wall. The temperature in this enclosure was controlled by a system consisting of a thermostat, relay switch, variac and heaters with a radiation shield (Figures 6 and 10). Two fans were used to circulate the air and create a uniform surface coefficient over the cold surface of the wall.

The Temperature Control System

The function of the temperature control system was to maintain equal temperatures in the guard and test section. As shown in Figure 7, sensing elements of a bridge system were placed in the guard and test sections. These resistors were extremely sensitive to temperature changes. The difference in the resistances of the elements caused by a temperature difference between the test and

guard sections, produced an unbalanced bridge system. This lack of balance induced a small voltage between the motor potentiometer wiper and the ground, that is, across the input terminals of the relay (Figure 8). In the event that the guard section temperature was higher, the relay would identify the signal voltage as due to an increase in the resistance of T3, and close the relay contacts between terminals one and three. This closed the circuit of the counter-clockwise winding, and started the motor. As the motor turned counter-clockwise, the motor potentiometer wiper moved towards the "G" end of the winding until the balance of the bridge circuit was restored. The relay then broke the contact and stopped the motor. The shaft of the motor was connected to the handle of a variac, and as the motor turned, it reduced the output voltage of the variac, and decreased the power supplied to the guard section heaters. With the output voltage of the variac reduced, the temperature in the guard section fell below that in the test section. This activated the control and turned the motor in the clockwise direction, causing an increase in the power supplied to the heaters, and restoring the temperature balance. As the motor turned from the maximum counter-clockwise position to the maximum clockwise position, the output voltage of the variac ranged from 35 to 110 volts. This cyclic control caused a maximum variation of 0.2 deg. F. in the steady state temperature in the test section.

The Thermocouples

Thermocouples were used to measure the temperatures in the regions of one, two and three dimensional heat flow, and to check the operation of the control system. Copper-constantan thermocouples were selected with the large gauge number of 30 in order to minimize the mass of wire in the wall, since approximately 120 thermocouples were installed. They were connected through a switch box to a 16 point recorder, which automatically converted the output of the transducers to degrees Fahrenheit (Figure 9). Each thermocouple was soldered to one of the 16 locations on one of the 10 connector plugs mounted in the switch box. The terminals of the recorder were soldered to a male plug which could be attached to any one of the female connectors thereby enabling the recorder to measure the temperatures in any one of the three regions of heat flow. The multiple point recorder measured the output of one of the thermocouples every 15 seconds with an accuracy of 0.2 deg.F.

The relaxation method was used with estimated physical properties of the wall materials to determine the temperature profiles on a plane normal to the axis of a component of the frame.[4] These temperature profiles were used as a guide to locate the thermocouples

4. W. H. Giedt, Principles of Engineering Heat Transfer, New York, D.Van Nostrand Co. Inc., 1957, pp 65-71.

in the wall. The thermocouple leads were taken along isothermal lines for two inches before branching away from the wall. This prevented heat conduction from the hot junction, along the wire, causing an error in temperature measurement.

Thermocouples were placed in the guard and test section air enclosures in order to check the operation of the temperature control system. Five thermocouples in the guard section were connected in parallel, and their signal was read on a potentiometer. This reading was compared with the output of a thermocouple located in the test section and when the average value of each signal was equal, the controls were functioning properly.

TEST PROCEDURE

Preparation for the Test

The fans and the control system were started and the control point adjustment was set at the maximum position. This caused the variac to supply the maximum voltage to the control heaters in the guard section. All of the heater circuits were then closed to give maximum heating. One or both of the heater circuits in the test section was closed, and the variac was set to give the voltage required for a particular temperature drop across the wall. For the tests performed in this study, the six ohm heater was used, and the variac was set at four volts to give a temperature difference across the wall of approximately 56 deg.F.

The thermostat in the exit section was set to the desired position, approximately 20 deg.F. above room temperature. As the room temperature varied between 70 deg.F. and 90 deg.F., the thermostat was set at 95 deg.F. and the heater circuits in the exit section were closed.

When the temperature in the test section was near the desired value, the control point setting was reduced in order to make the heating and cooling periods of the control heaters equal. With equal heating and cooling times, the apparatus was able to reach steady state, since the heat lost and gained by the test section air enclosure was equal during each control cycle. It was extremely difficult to both acquire and maintain the steady

state condition due to inadequate sensitivity in the control system. The control point setting was affected by the temperature difference between the guard section and the room, thus as the temperature in the apparatus approached the desired value, and as the room temperature changed, the control point had to be adjusted to maintain equal heating and cooling periods. When steady state had been obtained, the apparatus was ready for the test.

Performance of the Test

The temperatures were measured throughout the test section while the steady state existed in order to determine the initial temperatures for the theoretical analysis. Following this, several terminals in the recorder were attached directly to thermocouples in the two and three dimensional heat flow regions. The male connector was then attached to the connector with the thermocouples in the one dimensional region. Thus, the transient temperatures in the three areas of heat flow could be measured simultaneously throughout the test. The circuit of the test section heater was opened in order to begin the test.

During the test, the control point adjustment and the power supply to the guard section heaters were varied in order to prevent a temperature difference occuring between the hot air and the surface of the wall. This condition was maintained, as it corresponded to the assumption in the analysis that the heat capacity of the air

was negligible. A temperature difference was maintained across the wall of the test section air enclosure in order to prevent heat from flowing into the test section and causing a decrease in the cooling rate. This temperature difference was measured by a potentiometer, and was not allowed to become greater than 2 deg.F., as the temperature symmetries at the boundaries of the test section would be disturbed. This temperature drop was maintained by adjusting the control point and varying the heat supply.

If the temperature difference across the wall of the air enclosure became too large, the temperature of the air in the test section would become lower than the temperature in the wall's surface. This would cause heat to flow in the wrong direction and thus increase the cooling rate of the wall. In order to correct this situation, the control point setting must be raised Thus, two items were controlled simultaneously: (1) the temperature of the air in the test section, and (2) the temperature difference between the guard and test sections. Finally, when a temperature gradient no longer existed across the test wall, the test was terminated.

ANALYSIS

The numerical method of finite differences was used to determine the thermal response of the wall.[5] This was used because of the structure of the wall and the anisotropic properties of its materials.[6] There were several axes of temperature symmetry occuring at the centre of the fir members of the frame and at the midpoints between them (Figures 11 and 12). These axes of symmetry simplified the problem by making it possible to analyse only a small portion of the wall.

The heat flow was one, two and three dimensional owing to the presence of the fir frame. The two dimension heat flow at the studs and girts was due to the difference in the thermal conductivity of the fir and fibreglass insulation. The effect of a frame component on its surrounding temperature distribution did not extend beyond four inches from the centreline. Thus, as shown in Figure 12, there was a region enclosed by the studs and girts where the heat flow was one dimensional. Where the studs and girts intersected at right angles, the heat flow was three dimensional. At a sufficient distance away from the intersection, along a stud or girt, the temperature distribution on successive

---

5. G. M. Dusinberre, Numerical Analysis of Heat Flow, New York, McGraw-Hill Book Co. Inc., 1949.

6. Appendix B.

planes did not change, and the heat flow became two dimensional.

An analysis was performed neglecting the frame, in order to show its effect on the thermal response of the wall, and to obtain an approximate solution to the problem. This was a one dimensional heat flow analysis.

The exact analysis of the problem was performed on the region of three dimensional heat flow. The size of this region was chosen to make the boundaries the two dimensional heat flow regions and the corners the one dimensional regions.

The Exact Analysis

The small portion of the wall analysed in the exact analysis was divided into a grid for which the numerical equations were derived (Figure 13). Two important items had to be considered when this grid was selected: (1) the distance between the nodes had to be such that the heat flow between them was not falsely reduced due to high thermal resistances caused by large internodal distances, and (2) the number of nodes had to be such that the size of the problem was within the capacity of the computer available for the calculations. To satisfy both conditions, a grid system of 150 nodes was selected.

The derivation of the finite difference equations was based on the following assumptions:

(1) The contact resistances were negligible.
(2) The surface coefficients of heat transfer were uniform.
(3) The heat capacity of the air and apparatus components in the test section was negligible.
(4) The materials were homogeneous.
(5) The boundaries of the region were adiabatic.

The first assumption was based on the fact that the wall was constructed to minimize contact resistances. The surfaces of the 2 by 4 inch boards were smoothed by planing and the films of glue were made thin enough not to have any effect.[7] The second assumption was reasonable since fans were used to circulate the air over both sides of the wall. The heat capacity of the apparatus components in the test section was minimized by using light materials with low specific heats. The effect of the heat capacity of the air was shown to be negligible in an analysis by W. A. Wolfe.[8] The fourth assumption was good in the case of the hardboard, cedar and fir, as the variation in their specific weights was small. However, for the fibreglass insulation, which had a variation of 12.2 percent in its specific weight, the assumption was not as valid. It was reasonable however, since 12.2 percent variation was tolerable, and necessary since the variation in the

7. Brown and Marco, Introduction to Heat Transfer, McGraw Hill Book Co. Inc., 1958.

8. Wolfe, op. cit., p.23.

specific weight throughout the wall was not known. The fifth assumption was based on the fact that the temperature gradients normal to the boundaries were negligible (Figure 13).

Considering the law of conservation of energy, the following finite difference equation was written to express the heat flow at node 25a:[9]

$$\frac{k_{lh}\,x\,u}{4x}(T20a - T25a)dt + \frac{k_{lh}\,x\,u}{4x}(T24a - T25a)dt + \frac{k_h x^2}{u}(T25b - T25a)dt = \frac{\rho_h c_h x^2 u}{2}(T25a' - T25a)$$

The left side of the equation represents the heat flowing into and element during a time interval, dt, and the right side is the change in heat content during that time interval. Rearranging the above equation to solve for T25a'.

$$T25a' = \frac{\alpha_{lh}\,dt}{2x^2}(T20a + T24a) + \frac{2k_h\alpha_{lh}\,dt}{k_{lh}u^2}T25b + \left[1 - \left(2 + 4\frac{k_h x^2}{k_{lh}u^2}\right)\frac{\alpha_{lh}\,dt}{2x^2}\right]T25a$$

Substituting values and letting dt = 1 minute.

$$T25a' = 0.069\ T20a + 0.069\ T24a + 0.374\ T25b + 0.488\ T\ 25a$$

The coefficient of T25a was termed the self influence coefficient, since it affects its own future temperature. The self influence coefficient must be positive, otherwise an instability will arise in the equations.[10] This instability is produced by a thermodynamically impossible condition, where the future temperature

9. Dusinberre, op. cit., p. 115.

10. Ibid., p. 116.

at the end of the time interval, $d\tau$, will become lower as the temperature at the beginning of the interval becomes higher. Also, the coefficent should not equal zero, as this is equivalent to neglecting the heat capacty of the element and the node would then have no effect on its future temperatures. The most convenient time interval, which made all of the self influence coefficients positive was one minute. The equation for node 1a governed the selection of this time interval. The remaining 149 equations were derived in the same manner.[11]

The transient temperatures were calculated by substituting the initial temperatures into the equations, and calculating the temperatures at the end of the first time interval.

These temperatures became the initial values for the next time interval and the calculation was repeated. This procedure was continued until the temperature difference across the wall was negligible. The calculations were performed on the University of British Columbia's computer, ALWAC III E.

The initial temperatures were obtained by direct measurement, and by interpolating values from the curves drawn from the measured temperatures.[12]

The Approximate Analysis

The equation for one dimensional heat flow for node 25a

---

11. Appendix E.

12. Appendix F.

was simplified from the three dimensional case to:

$$\frac{k_h x^2}{u^2}(T25b - T25a)dt = \frac{\rho_h c_h x^2 u}{2}(T25a' - T25a)$$

rearranging terms and letting $M = \frac{u^2}{\alpha_h dt}$

The maximum value for dt was found by letting the self influence coefficient, $(1 - \frac{2}{M})$ equal zero.

Therefore, $M = 2$

and $dt = \frac{u^2}{2\alpha_h} = \frac{(.244)^2 (60)}{2(144)(0.00464)} = 2.67$ minutes

By arbitrarily letting dt = 2 minutes and substituting values the equation became:

$$T25a' = 0.748\ T25b + 0.252\ T25a$$

The equation for node 25b was:

$$\frac{k_h x^2}{u}(T25a - T25b)dt + \frac{k_i x^2}{u}(T25c - T25b)dt = \frac{x^2}{2}(u\rho_h c_h + v\rho_i c_i)(T25b' - t25a)$$

and reduced to:

$$T25b' = 0.572\ T25a + 0.054\ T25c + 0.374\ T25b$$

similarily,

$$T25c' = 0.116\ T25b + 0.116\ T25d + 0.768\ T25c$$

$$T25d' = 0.116\ T25c + 0.116\ T25e + 0.768\ T25d$$

$$T25e' = 0.040\ T25d + 0.130\ T25f + 0.830\ T25e$$

$$T25f' = 0.156\ T25e + 0.626\ To + 0.218\ T25f$$

The initial temperatures were measured and the calculations were performed,as in the exact analysis, on the ALWAC III E computer.

RESULTS

The theoretical and experimental results are in good agreement (Figures 17 and 20). The difference between the experimental results and the exact analysis was 14 percent and between the experimental results and the approximate analysis was 18 percent.

The theoretical and experimental results, when plotted on semi-logarithmic graph paper, showed the cooling of the wall was exponential (Figures 18 and 19). The approximate analysis showed a faster cooling rate than that predicted by the exact analysis, and the experimental curves exhibited a slower cooling rate for approximately the first ten hours than that shown by the theoretical results, and a faster cooling rate after the first ten hours.

The determination of the exact transient period for the wall was difficult, since the curves asymtotically approach zero, but the period was approximately 24 hours for an initial temperature difference across the wall of 55.6 deg. F. The agreement between the two tests indicated that the experimental results were consistent.

OBSERVATIONS AND CONCLUSIONS

The increase in the cooling rate of the experimental tests after approximately ten hours of cooling was due to heat being lost from the inside surface of the test wall to the guard section. This heat loss was caused by the lack of sensitivity in the control system, which allowed the test section air temperature to become lower than the temperature on the wall's surface. This poor control was caused by a combination of two characteristics of the apparatus: (1) a good thermal response between the quard and test sections and (2) the large temperature difference required between the two resistors to activate the relays. As the temperature in the guard section gradually fell during the cooling portion of a control cycle, the temperature in the test section readily followed it. Therefore, the temperature difference required to activate the controls occured after a long period of time. The time period required during the heating portion was shorter since the heating power was large enough to cause the guard section temperature to rise rapidly above the test section temperature. Thus, more heat was lost than added during a control cycle. Insulation was added to the wall of the test section in and effort to reduce the thermal response, but the reduction produced was not sufficient. Too much insulation could not be

added as it would increase the heat capacty of the test section, thereby slowing down the cooling of the wall.

The cooling was exponential for the first nine hours of test one, but afterwards the slope of the curve gradually increased because of the poor control (Figure 19). The straight portion of the the curve was extrapolated and new temperatures were obtained. The same was done to the second experimental curve which showed a sudden change after ten hours of cooling. The values obtained from the extrapolated portions were plotted and the resulting curves exhibited very good agreement (Figure 20). These new curves were more realistic as they allowed for the heat lost from the inner surface of the wall. As these curves are exponential, they may be expressed by the equation:

$$T - To = (Ti - To)\, e^{-t/\tau}$$

where τ , the time constant, depends only on the characteristics of the wall. The average value of τ obtained from the slope of the logarithmic curves was 6.334 hours. Thus, the equation can be used to determine the cooling of the wall for any initial temperature difference across the wall.

The difference between the experimental and theorectical results were attributed largely to the non-homogeneity of the

materials, particularily in the case of the insulation where the variation in the specific weight was 12.2 percent. The effect of any contact resistances and of the heat capacity of the test section would be to slow down the cooling rate in the tests. Although this effect was indeterminate, it was probably small owing to the careful construction of the apparatus. It was likely that the surface coefficient of heat transfer on the cool side of the wall was not uniform since the two fans were not capable of producing uniform air circulation over the entire surface of the wall. The surface coefficient would be lower in the regions where the air movement was less over the surface. Thus, the actual mean value of the coefficient was less than the value used, since the value of the coefficient could only be measured in the region of one dimensional heat flow, where the air circulation was good. All of these factors would cause the experimental cooling rate to be less than the theoretical rate.

Inaccuracies in the thermocouples would account for some of the difference between theory and experiment. However, this error is not likely to be more than two percent since calibration of the thermocouples showed errors of 1.5 deg. F. and less in 100 deg. F readings. It is possible that thermocouples may become loose after installation and cause large errors. However, no indication of this was observed on temperature records, but detection would be difficult if thermocouples detached between tests.

The agreement between the exerimental and theoretical curves was good and therefore indicated that the method of analysis was satisfactory. The results of the exact analysis showed a slower cooling rate than the one predicted by the approximate analysis. This was due to the fir having a lower thermal diffusivity than the insulation. The approximate analysis would be acceptable for walls with a smaller ratio of frame area to total surface area. The ratio for the wall studied was 1.0 to 9.6. However, the approximate analysis could be justified for this wall and other walls with similar frames since: (1) the maximum temperature difference between the one dimensional analysis and the three dimensional analyis was only four percent of the initial temperature difference across the wall, and (2) the one dimensional analysis was less laborious than the exact analysis. The exact analysis was very lengthy owing to the large number of equations derived and the large amount of computer time required.

Thus, the results indicated the following:

(1) The method of analysis and experimental work was satisfactory.

(2) The approximate analysis, which neglects the effect of the frame, gives sufficiently accurate results for walls with small ratios of frame area to surface area.

(3) The cooling of this type of wall can be represented by the equation $T = Ti\ e^{-t/\tau}$, where $\tau = 6.334$ hours for the wall investigated in this thesis.

(4) The control system used was not adequate and should be improved if more tests are to be conducted.

BIBLIOGRAPHY

Brown and Marco, Intoduction to Heat Transfer, New York, McGraw-Hill Book Co. Inc., 1958.

Batchelor, G. K., "Heat Transfer by Free Convection Across a Closed Cavity Between Vertical Boundaries at Different Temperatures", Quarterly of Applied Mathematics, 12: No. 3, October, 1954.

Campbell, W. G., Form and Style in Thesis Writing, Boston, Houghton Mifflin Co., 1954

Dussinberre, G. M., Numerical Analysis of Heat Flow, New York, McGraw-Hill Book Co. Inc., 1949.

Giedt, W. H., Principles of Engineering Heat Transfer, New York, D. Van Nostrand Co. Inc., 1957.

Kollmann, F., Technologie Des Holzes und der Holzwerkstoffe, Berlin, Springer, Vol.I, 1951.

MacLean, J. D., "Thermal Conductivity of Wood", Heating, Piping, and Air Conditioning, Vol.III, No. 6, June, 1941.

MacLean, J. D., "Rate of Disintegration of Wood Under Different Heating Conditions", Proceedings of American Wood-Preservers Assoc., 47:155-68, 1951.

Smith, E. G., "A Simple and Rigourous Method for the Determination of Heat Requirements of Simple Intermittently Heated Exterior Walls", Journal of Applied Physics, 12:638-642, 1941.

Tiemann, H. D., Wood Technology, New York, Pitman Publishing Corp., 1951.

United States Department of Agriculture, Forest Products Laboratory, Forest Service, Wood Handbook, No. 72, 1955.

United States Department of Agriculture, Forest Products Laboratory, Forest Service, The Rate of Temperature Changes in Wood Panels Heated Between Hot Plates, No. 1299, June, 1955.

Wolfe, W. A. "Transient Response of Heated Air in an Enclosure with Heat Losses", Journal of Heat Transfer, 81: 19-23, February, 1959.

APPENDIX

APPENDIX A. LIST OF SYMBOLS

A	area, $ft.^2$
C	specific heat of wet wood, B.T.U./lb. deg. F.
C_c	specific heat of cedar, B.T.U./lb. deg. F.
C_f	specific heat of fir, B.T.U./lb. deg. F.
C_h	specific heat of hardboard, B.T.U./lb. deg. F.
C_i	specific heat of fibreglass insulation, B.T.U./lb. deg. F.
Cm	mean specific heat of dry wood, B.T.U./lb. deg. F.
Cp	specific heat of dry wood, B.T.U./lb. deg. F.
D	weight after oven-drying.
dT	increment of temperature.
dt	increment of time.
dTx-y	temperature difference between planes x and y.
dx	increment of length.
e	base of natural logarithms.
h	surface coefficient of heat transfer for the hot surface, B.T.U./hr. $ft.^2$ deg. F.
h_o	surface coefficient of heat transfer for the cold surface, B.T.U./hr. $ft.^2$ deg. F.
k	thermal conductivity, B.T.U./in./hr. $ft.^2$ deg. F.
k_c	thermal conductivity of cedar tangential and normal to the grain, B.T.U./hr. ft. deg. F.
k_f	thermal conductivity of fir normal and tangential to the grain, B.T.U./hr. ft. deg. F.
k_h	thermal conductivity of hardboard normal to the plane of the hardboard, B.T.U./hr. ft. deg. F.
k_i	thermal conductivity of fibreglass insulation, B.T.U./hr.ft. deg. F.

$k_{\ell c}$ thermal conductivity of cedar parallel to the grain, B.T.U./hr. ft. deg. F.

$k_{\ell f}$ thermal conductivity of fir parallel to the grain, B.T.U./hr. ft. deg. F.

$k_{\ell h}$ thermal conductivity of the hardboard in the plane of the hardboard, B.T.U./hr. ft. deg. F.

ln natural logarithm.

M moisture content, percent.

M.V.x thermocouple reading at plane x, millivolts, m.v.

Q heat flux, B.T.U./hr $ft.^2$

S specific gravity of wood based on volume at current moisture content and weight when oven dried.

t time, hr.

T temperature, deg. F.

Ti initial hot surface temperature, deg. F.

To cold air temperature, deg. F.

T temperature of surrounding fluid, deg. F.

W original wet weight.

x cartesian coordinate

α thermal diffusivity, k/ c, $ft.^2/hr.$

α_c thermal diffusivity of cedar normal and tangential to the grain, $ft.^2/hr.$

α_f thermal diffusivity of fir normal and tangential to the grain, $ft.^2/hr.$

α_h thermal diffusivity of hardboard normal to the plane of the hardboard, $ft.^2/hr.$

α_i thermal diffusivity of fibreglass insulation, $ft.^2/hr.$

$\alpha_{\ell c}$ thermal diffusivity of cedar parallel to the grain, $ft.^2/hr.$

$\alpha_{\ell f}$ thermal diffusivity of fir parallel to the grain, $ft.^2/hr.$

α_{lh} thermal diffusivity of hardboard in the plane of the hardboard, ft.^{2}/hr.

β millivolt equivalent, m.v./deg. F.

ρ specific weight, lb./ft.^{3}

ρ_c specific weight of cedar, lb./ft.^{3}

ρ_f specific weight of fir, lb./ft.^{3}

ρ_h specific weight of hardboard, lb./ft.^{3}

ρ_i specific weight of fibreglass insulation, lb./ft.^{3}

τ time constant of wall, hr.

APPENDIX B. GENERAL PHYSICAL PROPERTIES OF WOOD AND OTHER WALL MATERIALS

General Properties of Wood

A. Thermal Conductivity

The thermal conductivity of wood is affected by:

(a) the direction of the grain
(b) the specific gravity
(c) the moisture content and its distribution
(d) structural characteristics
(e) heat
(f) temperature

(a) The Direction of the Grain

The thermal conductivity in the radial and tangential directions is approximately the same, but it is generally 2.25 to 2.75 times greater along the grain than in the transverse directions (Figure 14).[13] Thus, wood is an anisotropic material.

(b) The Specific Gravity

The thermal conductivity increases with the specific gravity. Temperature varies more slowly in woods with a high specific gravity than it does in woods with a low specific gravity. This is due to the increase in the specific heat per unit volume being greater than the increase in the thermal conductivity. Thus, the thermal diffusivity generally decreases as the specific gravity increases.

---

13. United States Department of Agriculture, Forest Products Laboratory, Forest Service, Wood Handbook, No. 72, 1955.

(c) The Moisture Content and Its Distribution

The thermal conductivity of wood can be calculated from the following formula when the moisture content is less than 40 percent.[14]

$$k = S\ (1.39 + 0.028M) + 0.165$$

The moisture content is defined by the equation $M = (\frac{W - D}{D})100$. The above equation for thermal conductivity applies to the wood in the wall, since the moisture content was about seven percent. It can be observed from the equation that the conductivity increases with an increase in the water content.

When the heating medium is below the boiling point of water, there is no significant difference in the rate of heating wood at different moisture contents ranging up to approximately 20 percent.[15] The moisture content affects the rate of temperature rise at heating temperatures well above 212 deg. F., since part of the heat entering the wood evaporates the water. Thus, the heating medium in the apparatus was never permitted to reach a temperature of 212 deg. F.

Studies of moisture distrubution have shown that when wood with a uniform moisture content was subjected to a

---

14. United States Department of Agriculture, Forest Products Laboratory, Forest Service, Wood Handbook, No. 72, 1955.

15. United States Department of Agriculture, Forest Products Laboratory, Forest Service, The Rate of Temperature Changes in Wood Panels Heated Between Hot Plates, No. 1299, June, 1955.

temperature gradient, there were often marked increases in the moisture content near the cold side of the specimen.[16] These variations in moisture distribution were due to differences in vapour pressure produced by the difference in temperatures. The variation was mainly influenced by the original amount of water in the wood and by the magnitude of the temperature gradient between the faces of the specimen. These studies have also shown that the changes in moisture distribution were comparatively small when the average initial moisture content was approximately ten percent or less.

There was only a small temperature gradient across the cedar and the hardboard in the wall of the transient heat transfer apparatus, and the moisture content in both was under ten percent. Thus, the change in the thermal conductivity of the hardboard and cedar due to the variation in the moisture distribution was negligible. The fir boards had large temperature gradients across then, but since they had a moisture content of approximately six percent, the effect of a non-uniform moisture content was again negligible.

(d) Structural Characteristics

Knots, checks, and cross grain structure have no appreciable effect on the conductivity of wood when they

---

16. J. D. MacLean, "Thermal Conductivity of Wood", Heating, Piping, and Air Conditioning, Vol.III, No. 6, June, 1941.

are not numerous.[17] Large knots have a tendency to increase the conductivity, and small checks have little or not effect. Wood with pronounced cross grain has an increased conductivity in the direction of the cross grain.

(e) Heat

It was found by J. D. MacLean that the effect of heat on the physical properties of wood depends upon several factors which include the temperature to which the wood is exposed, and the time the temperature is maintained.[18] The oven dry weight decreases if wood is subjected to a high temperature for a long period of time because of charring. The rate and amount of this decrease depends upon the temperature. The average reduction in the oven dry weight of wood was found to be 2.7 percent for a heating period of one year, and a temperature of 200 deg. F. These results indicated that the temperature should not be appreciably higher than 150 deg. F. if a good service life is desire.

(f) Temperature

There is a slight increase in the thermal conductivity with an increase in the average wood temperature. It was found in conductivity tests by J. D. MacLean that the conductivity varied from nearly zero to a maximum value of less than four

---

17. MacLean, op. cit.

18. J. D. Maclean, "Rate of Disintegration of Wood Under Different Heating Conditions", Proceedings of American Wood-Preservers Assoc., 47: 155-68, 1951.

percent with temperature differences across a specimen ranging from 22 deg. F. to 96 deg. F. Thus, the effect of the temperature on the thermal conductivity may be neglected since the largest temperature difference across any board was 40 deg. F.

B. Specific Weight

The specific weight of wood of any species varies considerably from tree to tree and even within the same tree.[19] There is usually considerable variation in the specific weight of the veneer cut from a single log. Thus, wood is generally a non-homogenous material.

C. Specific Heat

The specific heat varies with temperature according to the following formula:[20]

$$Cp = 0.266 + 0.000644(T - 32)$$

The average specific heat over a particular temperature interval is given by:

$$Cm = \frac{1}{T_2 - T_1} \int_{T_1}^{T_2} Cp \, dT$$

The specific heat is nearly independent of the specific gravity. The moisture content has a marked effect on the specific heat, since the specific heat of wood is close to that

19. United States Department of Agriculture, Forest Products Laboratory, Forest Service, The Rate of Temperature Changes in Wood Panels Heated Between Hot Plates, No. 1299, June, 1955.

20. F. Kollmann, Technologie Des Holzes und der Holzwerkstoffe, Berlin, Springer, Vol.I, 1951.

of air at 32 deg. F. The average specific heat which now includes the moisture content is given by: $C = \frac{M/100 + Cm}{M/100 + 1}$

Specific Properties of Individual Wall Materials

A. Fir and Cedar Boards

The species of the wood used in the wall were fir and cedar. All of the boards of both species were chosen with a straight grain running lengthwise along the board and parallel to the edge. They were also chosen free of knots and checks and were oven dried. Since the thermal conductivities in the radial and tangential directions are nearly equal, it was assumed that the thermal conductivity across the board and through the board were equal (Figure 14).

Both species of wood were assumed to be homogeneous in the analysis as the varation in the specific gravity of the cedar was 4.3 percent and of the fir was 6.9 percent as determined by tests.[21]

B. Hardboard

The hardboard is a fibrous material with wooden fibres randomly oriented in the plane of the hardboard. Thus, the hardboard is also an anisotropic material. The conductivity in any direction in the plane of the hardboard was assumed to be equal but the conductivity through the hardboard was less since the heat flowing through it crossed the grain.

---

21. Appendix C.

The hardboard was assumed to be homogeneous since the variation in the specific weight of the samples was only 2.5 percent. The specific heat cannot be calculated by the formula used for wood, since the hardboard fibres are bonded together by glue.

C. Fibreglass Insulation

The fibreglass insulation was assumed to be an isotropic material since it did not appear to have any directional properties. The insulation was treated as a homogeneous material although the variation in the specific weight of the samples from the average value was 12.5 percent.

APPENDIX C. DETERMINATION OF THE PHYSICAL PROPERTIES OF THE WALL MATERIALS

Steady State Determination of k_h, k_i, k_c, k_f, h_o and h

The properties k_h, k_i, k_c, and k_f, and the surface coefficients h_o and h were determined by a steady state temperature analysis of the wall. The heat flux was measured at the centre of the one dimensional heat flow region with a heat transducer. The D. C. millivlolt signal from the transducer was amplified and then recorded on an oscillograph. The average signal was determined by evaluating the area under the curve with a planimeter, and dividing the area by the base length. The average millivolt signal was then converted to units of heat flux by using a calibration curve and conversion factor supplied by the manufacturer. The temperature differences were measured across the hardboard, fibreglass insulation, and cedar by thermocouples.

The conductivities k_h, k_i, and k_c were then calculated from Fourier's equation. Using the data from test one and the following equations:[22]

$$k = Q \frac{dx}{dT}$$

$$dT_{a-b} = \frac{M.V.a - M.V.b}{\beta}$$

for cedar, $dT = \frac{.652 - .547}{.023} = 4.56$ deg. F.

for insulation, $dT = \frac{1.735 - .652}{.024} = 45.13$ deg. F.

for hardboard, $dT = \frac{1.763 - 1.735}{.0245} = 1.14$ deg. F.

---

22. Appendix F.

for cedar, dx = 0.75 inches

for insulation, dx = 3.25 inches

for hardboard, dx = 0.244 inches

Thus, k_c = 0.0633 B.T.U./hr. ft. deg. F.

k_i = 0.0277 B.T.U./hr. ft. deg. F.

k_h = 0.0844 B.T.U./hr. ft. deg. F.

The average value determined for k_i from tests one to seven was 0.0282 B.T.U./hr. ft. deg. F. with a deviation of 2.8 percent. Since the variation was very small, the average temperature gradient across the insulation was used to determine the heat flux for tests eight,nine, and ten.

The temperature difference across the convection film on the inside surface was measured and the surface coefficient was calculated from Newton's equation for surface convection.

$$h = \frac{Q}{dT}$$

From test one, $dT = \frac{1.819 - 1.763}{.0245} = 2.29$ deg. F.

$$h = \frac{4.62}{2.29} = 2.02 \text{ B.T.U./hr. ft.}^2$$

The average temperature difference across the convection film on the outside surface was determined by evaluating the average height of the curve given by a trace of the temperature difference on an oscillograph. This average temperature difference and heat

flux given by tests 11 to 20 determined the outside surface coefficient, h_o.[23]

The heat flow was one dimensional along the centreline of a frame component since the temperature distribution was symmetric about the centre axis (Figure 11). Thus, the temperature differences were measured across the hardboard, fir and cedar at the centreline of a fir board. The heat flux was determined by using the previously calculated conductivites of the hardboard and cedar. The conductivity, k_f, was then evaluated.

This method of determining the conductivities and surface coefficients appeared to be reliable, since the calculated value of k_h agreed within one percent of the manufacturer's value. The average physical properties were tabulated in Appendix D.

Steady State Oven Tests to Determine $k_{\ell h}$, $k_{\ell c}$, and $k_{\ell f}$

In order to obtain $k_{\ell h}$, $k_{\ell c}$, and $k_{\ell f}$, it was necessary to test specimens with the heat flowing parallel to the grain. Specimens were mounted in a plywood frame and placed in the doorway of an oven with the grain oriented perpendicular to the plane of the door (Figure 15). The oven air was well circulated by a fan to produce a uniform surface coefficent. The dimensions, heat flow, and temperature difference for each specimen were

23. Appendix F.

measured and the longitudinal conductivity was calculated from Fourier's equation. The heat flow was determined by using a heat flux transducer as described on page 34 of this appendix.

Determination of the Specific Weight and Moisture Content

The volume and the wet weight, which is defined as the weight under current moisture content, was measured for each specimen removed from the cedar and fir boards. These samples were oven dried for 24 hours at a temperature of 105 deg. C. and weighed. From these values the moisture contents were calculated.

Since the moisture content of the wall materials was expected to be reduced by the higher temperatures in the apparatus, the moisture content of some cedar samples was determined after they were subjected to the higher temperatures. Tests one to eight for moisture content were made on the cedar samples not subjected to the conditions in the apparatus and tests nine to twelve were performed on specimens subjected to the temperatures. It was impossible to measure the moisture content of the fir under test conditions since it was an interior wall material. However, the moisture content of the fir was considered negligible, as the initial moisture contents of the fir and cedar were approximately equal and since the fir was subjected to test temperatures of 117 deg. F. to 160 deg. F. while the cedar was subjected to lower temperatures of 107 deg. F. to 117 deg. F. and had a moisture

content of only 4.22 percent. The moisture content of the hardboard was also considered insignificant since it was subjected to an average temperature of 161 deg. F.

The specific weight of the hardboard, cedar, and fir was based on the oven dried weight. The specific weight of the hardboard was 55.92 lb./ft.^{3} with a variation of 2.7 percent, and the cedar was 20.22 lb./ft.^{3} with a variation of 3.5 percent. The specific weight of the fibreglass insulation was 4 lb./ft.^{3} but it was compressed to a thickness of 3.25 inches in the wall and thereby increased its specific weight to 4.92 lb./ft.^{3} The variation in the weight of the insulation was 12.2 percent.

Determination of Specific Heat

The specific heat of the fir was calculated from the following equation, since the moisture content was considered negligible.[24]

$$C_f = \frac{1}{160 - 90} \int_{90}^{160} [0.266 + 0.000644(T - 32)]dT$$

$$= 0.320 \text{ B.T.U./lb. deg. F.}$$

For the cedar with a moisture content of 4.22 percent and at an average temperature of 105 deg. F. the following method was used:

$$C_c = \frac{M/100 + Cp}{M/100 + 1} = \frac{.0422 + .266 + .000644(105 - 32)}{1.0422}$$

$$= 0.341 \text{ B.T.U./lb. deg. F.}$$

24. Appendix B.

The specific heat of the fibreglass insulation was stated by the manufacturer to be 0.20 B.T.U./lb. deg. F. The specific heat of the hardboard was found to be 0.255 B.T.U./lb deg. F. in the following section of this appendix.

Determination of the Thermal Diffusivity of Hardboard

The thermal diffusivity of the hardboard was found directly by experiment. The experiment was based upon the following analysis which showed that the slope of the transient cooling curve, plotted on semi-logarithmic graph paper, for a point at the midpoint of a plate was related to the thermal diffusivity.[25] The following assumtions were made for a plate of thickness, 2ℓ, which was assumed to be homogenous.

(a) $\frac{d}{dx}(T - T_\infty) = 0$ at $x = 0$, the centre of the plate

(b) h is very large, such that k/h tends to zero

(c) $-k\frac{d}{dx}(T - T_\infty) = h\,(T - T_\infty)$ at $x = \ell$

(d) $T - T_\infty = Ti - T_\infty$ at $t = 0$

(e) the solution is of the form $T(x,t) = X(x)\,T(t)$

Applying (e) to the heat diffusion equation:

$$\frac{\partial T}{\partial t} = \alpha \frac{\partial^2 T}{\partial x^2}$$

the following solution was obtained:

$$T - T_\infty = e^{-m^2 \alpha t}\,[\,C_1 \cos mx + C_2 \sin mx]$$

from (a) $C_2 = 0$

25. Giedt, op. cit., pp. 293 - 297.

from (c) $k\, e^{-m^2\alpha t} C_1 \sin m\ell = h\, e^{-m^2\alpha t} C_1 \cos m\ell$

thus $\cot m\ell = mk/h$

from (b) $\cot m\ell = 0$ and $m = (\frac{2n+1}{2})\ \frac{\pi}{\ell}$

Upon considering (d), the solution becomes:

$$\frac{T - T_\infty}{Ti - T_\infty} = \sum_{n=0}^{\infty} C_n e^{-\left(\frac{2n+1}{2}\right)^2 \frac{\pi^2 \alpha}{\ell^2} t} \cos\left(\frac{2n+1}{2}\right) \frac{\pi}{\ell} x$$

Now, as t becomes large, terms with $n \geq 1$ are negligible as compared to the $n=0$ term. Thus, by taking the natural logarithm of both sides when t is large

$$\ln (T - T_\infty) - \ln (Ti - T_\infty) = \ln C_0 - \frac{\pi^2 \alpha}{4\ell^2} t$$

For a thermocouple, the voltage, M.V., is proportional to the temperature difference for a finite range. Thus

$$\ln (M.V. - M.V._\infty) = - \frac{\pi^2 \alpha}{4\ell^2} t$$

When the natural logarithm of $(M.V. - M.V._\infty)$ is plotted against time, the slope of the line is equal to $- \frac{\pi^2 \alpha}{4\ell^2}$

Two sheets of hardboard, six inches square, were glued together with a thermocouple at the centre of the interface. The effect of the heat loss at the edges was negligible since the ratio of the length of the sides to the thickness was large. The ratio was approximately twelve to one. The plate was waterproofed with a coating of varnish, which was made as thin as possible in order to minimize the effect of the varnish on the diffusivity. The specimen was heated to a uniform temperature and immersed in a cold stream of water. The flow was made as large

as possible in order to achieve assumption (b). The cooling temperatures were measured on a potentiometer and plotted.

From the first experiment (Figure 16):

$$\ell = 0.25 \text{ inches}$$

$$\text{M.V.} - \text{M.V.}_{\infty} = 0.309 \text{ m.v. at } t = 5 \text{ minutes}$$

$$\text{M.V.} - \text{M.V.}_{\infty} = 0.016 \text{ m.v. at } t = 11.75 \text{ minutes}$$

and solving the above equation for

$$\frac{\log. 0.309 - \log. 0.016}{11.75 - 5.0} = \frac{\pi^2 \alpha}{4(2.303)(.25)^2}$$

$$= 17.142 \alpha$$

Thus, $\alpha_h = 0.00463$ ft.^{2}/hr.

Also, $C_h = k_h / \rho_h \alpha_h = 0.255$ B.T.U./lb. deg. F.

From the second experiment,

$$\ell = 0.25 \text{ inches}$$

$$\text{M.V.} - \text{M.V.}_{\infty} = 0.478 \text{ m.v. at } t = 4.0 \text{ minutes}$$

$$\text{M.v.} - \text{M.V.}_{\infty} = 0.082 \text{ m.v. at } t = 8.0 \text{ minutes}$$

Thus, $\alpha_h = 0.00465$ ft.^{2}/hr.

and $C_h = 0.254$ B.T.U./lb. deg. F.

The average values used were:

$$\alpha_h = 0.00464 \text{ ft.}^2/\text{hr.}$$

$$C_h = 0.255 \text{ B.T.U./lb. deg. F.}$$

APPENDIX D. PHYSICAL PROPERTIES OF THE WALL MATERIALS

c_c = 0.341 B.T.U./lb. deg. F.

c_f = 0.320 B.T.U./lb. deg. F.

c_h = 0.255 B.T.U./lb. deg. F.

c_i = 0.20 B.T.U./lb. deg. F.

k_c = 0.063 B.T.U./hr. ft. deg. F.

k_f = 0.061 B.T.U./hr. ft. deg. F.

k_h = 0.066 B.T.U./hr. ft. deg. F.

k_i = 0.028 B.T.U./hr. ft. deg. F.

$k_{\ell c}$ = 0.147 B.T.U./hr. ft. deg. F.

$k_{\ell f}$ = 0.301 B.T.U./hr. ft. deg. F.

$k_{\ell h}$ = 0.326 B.T.U./hr. ft. deg. F.

h = 2.02 B.T.U./hr. $ft.^2$ deg. F.

h_o = 4.04 B.T.U./hr. $ft.^2$ deg. F.

α_c = 0.00914 $ft.^2$/hr.

α_f = 0.00543 $ft.^2$/hr.

α_h = 0.00464 $ft.^2$/hr.

α_i = 0.0284 $ft.^2$/hr.

$\alpha_{\ell c}$ = 0.0213 $ft.^2$/hr.

$\alpha_{\ell f}$ = 0.0268 $ft.^2$/hr.

$\alpha_{\ell h}$ = 0.0229 $ft.^2$/hr.

ρ_c = 20.22 lb./$ft.^3$

ρ_f = 35.07 lb./$ft.^3$

ρ_h = 55.92 lb./$ft.^3$

ρ_i = 4.92 lb./$ft.^3$

APPENDIX E. SUMMARY OF THEORETICAL EQUATIONS

$$T1a' = .273T2a + .273T6a + .373T1b + .081T1a$$

$$T2a' = .091T1a + .046T3a + .274T7a + .374T2b + .215T2a$$

$$T3a' = .034T2a + .034T4a + .275T8a + .375T3b + .282T3a$$

$$T4a' = .034T3a + .034T5a + .275T9a + .375T4b + .282T4a$$

$$T5a' = .069T4a + .274T10a + .374T5b + .283T5a$$

$$T6a' = .091T1a + .046T11a + .274T7a + .374T6b + .215T6a$$

$$T7a' = .091T6a + .091T2a + .046T8a + .046T12a + .374T7b + .352T7a$$

$$T8a' = .034T7a + .034T9a + .046T13a + .091T3a + .374T8b + .421T8a$$

$$T9a' = .034T8a + .034T10a + .046T14a + .091T4a + .374T9b + .421T9a$$

$$T10a' = .069T9a + .046T15a + .091T5a + .374T10b + .420T10a$$

$$T11a' = .034T6a + .034T16a + .275T12a + .374T11b + .283T11a$$

$$T12a' = .034T7a + .034T17a + .046T13a + .091T11a + .374T12b + .421T12a$$

$$T13a' = .034T8a + .034T12a + .034T14a + .034T18a + .374T13b + .490T13a$$

$$T14a' = .034T9a + .034T13a + .034T15a + .034T19a + .374T14b + .490T14a$$

$$T15a' = .069T14a + .034T10a + .034T20a + .374T15b + .489T15a$$

$$T16a' = .034T11a + .034T21a + .274T17a + .374T16b + .284T16a$$

$$T17a' = .034T12a + .034T22a + .046T18a + .091T16a + .374T17b + .421T17a$$

$$T18a' = .034T17a + .034T13a + .034T19a + .034T23a + .374T18b + .490T18a$$

$$T19a' = .034T18a + .034T14a + .034T20a + .034T24a + .374T19b + .490T19a$$

$$T20a' = .069T19a + .034T15a + .034T25a + .374T20b + .489T20a$$

$$T21a' = .069T16a + .274T22a + .374T21b + .283T21a$$

$$T22a' = .069T17a + .046T23a + .091T21a + .374T22b + .420T22a$$

$$T23a' = .069T18a + .034T22a + .034T24a + .374T23b + .489T23a$$

$$T24a' = .069T19a + .034T23a + .034T25a + .374T24b + .489T24a$$

$$T25a' = .069T20a + .069T24a + .374T25b + .488T25a$$

$$T1b' = .083T1a + .017T1c + .111T2b + .310T6b + .479T1b$$

$$T2b' = .083T2a + .017T2c + .037T1b + .052T3b + .178T7b + .633T2b$$

$$T3b' = .083T3a + .017T3c + .039T2b + .039T4b + .111T8b + .711T3b$$

$$T4b' = .083T4a + .017T4c + .039T3b + .039T5b + .111T9b + .711T4b$$

$$T5b' = .083T5a + .017T5c + .078T4b + .111T10b + .711T5b$$

$$T6b' = .083T6a + .017T6c + .111T7b + .103T1b + .052T11b + .634T6b$$

$$T7b' = .121T7a + .019T7c + .054T6b + .039T8b + .087T2b + .039T12b + .641T7b$$

$$T8b' = .158T8a + .021T8c + .038T9b + .038T7b + .071T3b + .027T13b + .647T8b$$

$$T9b' = .158T9a + .021T9c + .038T10b + .038T8b + .071T4b + .027T14b + .647T9b$$

$$T10b' = .158T10a + .021T10c + .071T5b + .076T9b + .027T15b + .647T10b$$

$$T11b' = .083T11a + .017T11c + .039T6b + .039T16b + .111T12b + .711T11b$$

$$T12b' = .158T12a + .021T12c + .038T17b + .038T7b + .071T11b + .027T13b + .647T12b$$

$$T13b' = .286T13a + .027T13c + .036T8b + .036T12b + .036T18b + .036T14b + .543T13b$$

$$T14b' = .286T14a + .027T14c + .036T9b + .036T13b + .036T19b + .036T15b + .543T14b$$

$$T15b' = .286T15a + .027T15c + .072T14b + .036T10b + .036T20b + .543T15b$$

$$T16b' = .083T16a + .017T16c + .039T11b + .039T21b + .111T17b + .711T16b$$

$$T17b' = .158T17a + .021T17c + .038T22b + .038T12b + .071T16b + .027T18b + .647T17b$$

$$T18b' = .286T18a + .027T18c + .036T13b + .036T17b + .036T23b + .036T19b + .543T18b$$

$$T19b' = .286T19a + .027T19c + .036T14b + .036T18b + .036T24b + .036T20b + .543T19b$$

$$T20b' = .286T20a + .027T20c + .072T19b + .036T15b + .036T25b + .543T20b$$

$$T21b' = .083T21a + .017T21c + .078T16b + .111T22b + .711T21b$$

$$T22b' = .158T22a + .021T22c + .071T21b + .072T17b + .027T23b + .647T22b$$

$$T23b' = .286T23a + .027T23c + .072T18b + .036T22b + .036T24b + .543T23b$$

$$T24b' = .286T24a + .027T24c + .072T19b + .036T23b + .036T25b + .543T24b$$

$$T25b' = .286T25a + .027T25c + .072T24b + .072T20b + .543T25b$$

$$T1c' = .011T1b + .011T1d + .065T2c + .321T6c + .592T1c$$

$$T2c' = .011T2b + .011T2d + .022T1c + .053T3c + .151T7c + .752T2c$$

$$T3c' = .011T3b + .011T3d + .040T2c + .040T4c + .065T8c + .833T3c$$

$$T4c' = .011T4b + .011T4d + .040T3c + .040T5c + .065T9c + .833T4c$$

$$T5c' = .011T5b + .011T5d + .080T4c + .065T10c + .833T5c$$

$$T6c' = .011T6b + .011T6d + .107T1c + .053T11c + .065T7c + .753T6c$$

$$T7c' = .014T7b + .014T7d + .180T6c + .084T2c + .036T8c + .036T12c + .636T7c$$

$$T8c' = .018T8b + .018T8d + .055T3c + .041T7c + .041T9c + .013T13c + .814T8c$$

$$T9c' = .018T9b + .018T9d + .055T4c + .041T8c + .041T10c + .013T14c + .814T9c$$

$$T10c' = .018T10b + .018T10d + .055T5c + .013T15c + .082T9c + .814T10c$$

$$T11c' = .011T11b + .011T11d + .040T6c + .040T16c + .065T12c + .833T11c$$

$$T12c' = .018T12b + .018T12d + .055T11c + .041T7c + .041T17c + .013T13c + .814T12c$$

$$T13c' = .058T13b + .058T13d + .043T8c + .043T14c + .043T18c + .043T12c + .712T13c$$

$$T14c' = .058T14b + .058T14d + .043T9c + .043T15c + .043T19c + .043T13c + .712T14c$$

$$T15c' = .058T15b + .058T15d + .086T14c + .043T10c + .043T20c + .712T15c$$

$$T16c' = .011T16b + .011T16d + .040T11c + .040T21c + .065T17c + .833T16c$$

$$T17c' = .018T17b + .018T17d + .055T16c + .041T12c + .041T22c + .013T18c + .814T17c$$

$$T18c' = .058T18b + .058T18d + .043T13c + .043T19c + .043T23c + .043T17c + .712T18c$$

$$T19c' = .058T19b + .058T19d + .043T14c + .043T20c + .043T24c + .043T18c + .712T19c$$

$$T20c' = .058T20b + .058T20d + .086T19c + .043T15c + .043T25c + .712T20c$$

$$T21c' = .011T21b + .011T21d + .080T16c + .065T22c + .833T21c$$

$$T22c' = .018T22b + .018T22d + .055T21c + .013T23c + .082T17c + .814T22c$$

$$T23c' = .058T23b + .058T23d + .086T18c + .043T22c + .043T24c + .712T23c$$

$$T24c' = .058T24b + .058T24d + .086T19c + .043T23c + .043T25c + .712T24c$$

$$T25c' = .058T25b + .058T25d + .086T20c + .086T24c + .712T25c$$

$$T1d' = .011T1c + .011T1e + .065T2d + .321T6d + .592T1d$$

$$T2d' = .011T2c + .011T2e + .022T1d + .053T3d + .151T7d + .752T2d$$

$$T3d' = .011T3c + .011T3e + .040T2d + .040T4d + .065T8d + .833T3d$$

$$T4d' = .011T4c + .011T4e + .040T3d + .040T5d + .065T9d + .833T4d$$

$$T5d' = .011T5c + .011T5e + .080T4d + .065T10d + .833T5d$$

$$T6d' = .011T6c + .011T6e + .107T1d + .053T11d + .065T7d + .753T6d$$

$$T7d' = .014T7c + .014T7e + .180T6d + .084T2d + .036T8d + .036T12d + .636T7d$$

$$T8d' = .018T8c + .018T8e + .055T3d + .041T7d + .041T9d + .013T13d + .814T8d$$

$$T9d' = .018T9c + .018T9e + .055T4d + .041T8d + .041T10d + .013T14d + .814T9d$$

$$T10d' = .018T10c + .018T10e + .055T5d + .013T15d + .082T9d + .814T10d$$

$$T11d' = .011T11c + .011T11e + .040T6d + .040T16d + .065T12d + .833T11d$$

$$T12d' = .018T12c + .018T12e + .055T11d + .041T7d + .041T17d + .013T13d + .814T12d$$

$$T13d' = .058T13c + .058T13e + .043T8d + .043T14d + .043T18d + .043T12d + .712T13d$$

$$T14d' = .058T14c + .058T14e + .043T9d + .043T15d + .043T19d + .043T13d + .712T14d$$

$$T15d' = .058T15c + .058T15e + .086T14d + .043T10d + .043T20d + .712T15d$$

$$T16d' = .011T16c + .011T16e + .040T11d + .040T21d + .065T17d + .833T16d$$

$$T17d' = .018T17c + .018T17e + .055T16d + .041T12d + .041T22d + .013T18d + .814T17d$$

$$T18d' = .058T18c + .058T18e + .043T13d + .043T19d + .043T23d + .043T17d + .712T18d$$

$$T19d' = .058T19c + .058T19e + .043T14d + .043T20d + .043T24d + .043T18d + .712T19d$$

$$T20d' = .058T20c + .058T20e + .086T19d + .043T15d + .043T25d + .712T20d$$

$$T21d' = .011T21c + .011T21e + .080T16d + .065T22d + .833T21d$$

$$T22d' = .018T22c + .018T22e + .055T21d + .013T23d + .082T17d + .814T22d$$

$$T23d' = .058T23c + .058T23e + .086T18d + .043T22d + .043T24d + .712T23d$$

$$T24d' = .058T24c + .058T24e + .086T19d + .043T23d + .043T25d + .712T24d$$

$$T25d' = .058T25c + .058T25e + .086T20d + .086T24d + .712T25d$$

$$T1e' = .015T1d + .023T1f + .122T2e + .258T6e + .582T1e$$

$$T2e' = .015T2d + .023T2f + .040T1e + .050T3e + .138T7e + .734T2e$$

$$T3e' = .015T3d + .023T3f + .037T2e + .037T4e + .078T8e + .810T3e$$

$$T4e' = .015T4d + .023T4f + .037T3e + .037T5e + .078T9e + .810T4e$$

$$T5e' = .015T5d + .023T5f + .074T4e + .078T10e + .810T5e$$

$$T6e' = .015T6d + .023T6f + .086T1e + .043T11e + .122T7e + .711T6e$$

$$T7e' = .017T7d + .025T7f + .064T2e + .057T6e + .038T8e + .028T12e + .771T7e$$

$$T8e' = .017T8d + .040T8f + .036T7e + .036T9e + .045T3e + .016T13e + .810T8e$$

$$T9e' = .017T9d + .040T9f + .036T8e + .036T10e + .045T4e + .016T14e + .810T9e$$

$$T10e' = .017T10d + .040T10f + .072T9e + .045T5e + .016T15e + .810T10e$$

$$T11e' = .015T11d + .023T11f + .032T6e + .032T16e + .122T12e + .776T11e$$

$$T12e' = .017T12d + .040T12f + .071T11e + .027T7e + .027T17e + .028T13e + .790T12e$$

$$T13e' = .020T13d + .065T13f + .034T12e + .034T14e + .019T8e + .019T18e + .809T13e$$

$$T14e' = .020T14d + .065T14f + .034T13e + .034T15e + .019T9e + .019T19e + .809T14e$$

$$T15e' = .020T15d + .065T15f + .068T14e + .019T10e + .019T20e + .809T15e$$

$$T16e' = .015T16d + .023T16f + .032T11e + .032T21e + .122T17e + .776T16e$$

$$T17e' = .017T17d + .040T17f + .071T16e + .027T12e + .027T22e + .028T18e + .790T17e$$

$$T18e' = .020T18d + .065T18f + .034T17e + .034T19e + .019T13e + .019T23e + .809T18e$$

$$T19e' = .020T19d + .065T19f + .034T18e + .034T20e + .019T14e + .019T24e + .809T19e$$

$$T20e' = .020T20d + .065T20f + .068T19e + .019T15e + .019T25e + .809T20e$$

$$T21e' = .015T21d + .023T21f + .065T16e + .122T22e + .775T21e$$

$$T22e' = .017T22d + .040T22f + .071T21e + .054T17e + .028T23e + .790T22e$$

$$T23e' = .020T23d + .065T23f + .034T22e + .034T24e + .038T18e + .809T23e$$

$$T24e' = .020T24d + .065T24f + .034T23e + .034T25e + .038T19e + .809T24e$$

$$T25e' = .020T25d + .065T25f + .038T20e + .068T24e + .809T25e$$

$$T1f' = .078T1e + .313To + .255T2f + .109T6f + .245T1f$$

$$T2f' = .078T2e + .313To + .085T1f + .042T3f + .109T7f + .373T2f$$

$$T3f' = .078T3e + .313To + .032T2f + .032T4f + .109T8f + .436T3f$$

$$T4f' = .078T4e + .313To + .032T3f + .032T5f + .109T9f + .436T4f$$

$$T5f' = .078T5e + .313To + .064T4f + .109T10f + .436T5f$$

$$T6f' = .078T6e + .313To + .037T1f + .018T11f + .255T7f + .299T6f$$

$$T7f' = .078T7e + .313To + .037T2f + .018T12f + .085T6f + .043T8f + .426T7f$$

$$T8f' = .078T8e + .313To + .032T7f + .032T9f + .037T3f + .018T13f + .490T8f$$

$$T9f' = .078T9e + .313To + .032T8f + .032T10f + .037T4f + .018T14f + .490T9f$$

$$T10f' = .078T10e + .313To + .037T5f + .018T15f + .064T9f + .490T10f$$

$$T11f' = .078T11e + .313To + .013T6f + .013T16f + .255T12f + .328T11f$$

$$T12f' = .078T12e + .313To + .085T11f + .043T13f + .014T7f + .014T17f + .453T12f$$

$$T13f' = .078T13e + .313To + .013T8f + .013T18f + .032T14f + .032T12f + .519T13f$$

$$T14f' = .078T14e + .313To + .013T9f + .013T19f + .032T15f + .032T13f + .519T14f$$

$$T15f' = .078T15e + .313To + .013T20f + .064T14f + .013T10f + .519T15f$$

$$T16f' = .078T16e + .313To + .013T21f + .255T17f + .013T11f + .328T16f$$

$$T17f' = .078T17e + .313To + .085T16f + .043T18f + .014T12f + .014T22f + .453T17f$$

$$T18f' = .078T18e + .313To + .013T13f + .013T23f + .032T19f + .032T17f + .519T18f$$

$$T19f' = .078T19e + .313To + .013T14f + .013T24f + .032T20f + .032T18f + .519T19f$$

$$T20f' = .078T20e + .313To + .064T19f + .013T15f + .013T25f + .519T20f$$

$$T21f' = .078T21e + .313To + .027T16f + .255T22f + .327T21f$$

$$T22f' = .078T22e + .313To + .027T17f + .085T21f + .043T23f + .454T22f$$

$$T23f' = .078T23e + .313To + .032T22f + .032T24f + .027T18f + .518T23f$$

$$T24f' = .078T24e + .313To + .032T23f + .032T25f + .027T19f + .518T24f$$

$$T25f' = .078T25e + .313To + .027T20f + .064T24f + .518T25f$$

APPENDIX F. DATA

Data to Determine h_o, h, k_4, k_c and k_i

Test	M.V.i	M.V.a	M.V.b	M.V.e	M.V.f	M.V.	Q
1	1.819	1.763	1.735	0.652	0.547		4.62
2	1.828	1.758	1.723	0.653	0.551		4.77
3	1.823	1.750	1.718	0.642	0.541		4.74
4	1.820	1.760	1.723	0.641	0.542		4.69
5	1.809	1.766	1.727	0.637	0.538		4.78
6	1.771	1.706	1.675	0.623	0.530		4.52
7	1.790	1.738	1.698	0.619	0.520		4.63
8		1.675	1.643	0.578	0.487		4.54
		1.667	1.627	0.554	0.457		4.54
		1.650	1.617	0.540	0.411		4.54
		1.654	1.617	0.538	0.427		4.54
		1.655	1.616	0.537	0.412		4.54
		1.653	1.616	0.537	0.434		4.54
		1.655	1.615	0.538	0.424		4.54
		1.656	1.618	0.543	0.445		4.54
		1.654	1.617	0.543	0.434		4.54
		1.656	1.619	0.546	0.453		4.54
9	1.688	1.638	1.600	0.540			4.49
	1.678	1.632	1.605	0.538			4.49
	1.688	1.637	1.605	0.538			4.49
	1.695	1.636	1.605	0.541			4.49
	1.697	1.635	1.603	0.538			4.49
	1.688	1.636	1.604	0.538			4.49
10					0.330	0.301	4.73
					0.329	0.303	4.73
					0.328	0.302	4.73
					0.326	0.300	4.73
					0.326	0.299	4.73
					0.326	0.296	4.73
					0.323	0.296	4.73
					0.321	0.293	4.73
					0.315	0.289	4.73
					0.309	0.280	4.73

Data to Determine k_f

Test	M.V.a	M.V.b	M.V.e	M.V.f
11	1.588	1.530	0.620	0.446
12	1.597	1.536	0.620	0.449
13	1.604	1.538	0.624	0.417
14	1.608	1.542	0.625	0.423
15	1.603	1.541	0.624	0.448
16	1.608	1.542	0.628	0.423
17	1.611	1.546	0.629	0.446
18	1.611	1.544	0.629	0.424
19	1.610	1.544	0.626	0.455
20	1.611	1.543	0.628	0.427
Average	1.605	1.540	0.625	0.435

Data from Oven Tests to Determine k_{lf}, k_{lc} and k_{lh}

Test	Average Inside Temp.	Average Outside Temp.	Q	dx
k_{lf}	170.12	139.96	151.89	0.716
	170.12	140.96	148.34	0.716
k_{lh}	182.31	148.00	209.39	0.668
	181.00	147.72	189.68	0.668
	184.73	151.21	192.45	0.668
k_{lc}	191.36	132.96	130.45	0.795
	192.88	131.67	134.95	0.795

Data for Moisture Content and Specific Weight of Fir and Cedar

Cedar

Test	Wet Weight	Dry Weight	% Moisture Content	Volume	Specific Gravity
	grams	grams		m.l.	
1	0.8248	0.774	6.59	2.426	0.319
2	0.8099	0.761	6.44	2.413	0.315
3	0.8536	0.802	6.48	2.433	0.330
4	0.8437	0.794	6.30	2.407	0.330
5	0.8502	0.799	6.38	2.420	0.330
6	0.8290	0.776	6.83	2.433	0.319
7	0.8760	0.814	7.62	2.407	0.338
8	1.8027	1.677	7.51	5.190	0.323
9	0.6860	0.659	4.10		
10	0.5910	0.567	4.23		
11	0.6180	0.591	4.57		
12	0.6810	0.655	3.97		

Fir

1	2.161	2.028	6.56	3.645	0.556
2	2.421	2.268	6.75	4.066	0.558
3	2.069	1.936	6.87	3.439	0.563
4	2.270	2.111	7.53	3.867	0.545
5	2.222	2.075	7.08	3.642	0.570
6	2.126	1.984	7.16	3.478	0.570
7	3.721	3.469	7.26	6.239	0.556
8	4.701	4.389	7.11	7.796	0.563
9	4.285	4.006	6.96	6.967	0.575
10	3.660	3.406	7.46	5.982	0.569

Specific Weight of Hardboard

Sample	Thickness inches	Length inches	Width inches	Volume $inches^3$	Weight grams	Specific Weight $lb./ft.^3$
1	0.245	1.985	2.007	0.976	14.33	55.92
2	0.244	2.009	2.011	0.986	14.30	55.24
3	0.244	2.010	2.012	0.987	14.42	55.65
4	0.245	2.008	2.011	0.989	14.73	56.73
5	0.243	2.009	1.998	0.975	14.59	57.00
6	0.245	1.987	2.007	0.977	14.36	55.98
7	0.244	1.993	2.011	0.978	14.23	55.42
8	0.243	2.003	2.010	0.978	14.00	54.53
9	0.244	2.011	2.011	0.987	14.35	55.38
10	0.246	2.013	2.011	0.996	14.76	56.45
11	0.246	2.010	2.011	0.994	14.81	56.75
12	0.243	1.998	2.011	0.976	14.32	55.89
13	0.244	2.008	2.008	0.984	14.46	55.97
14	0.245	2.006	2.011	0.988	14.55	56.09
15	0.246	2.010	2.008	0.993	14.54	55.77

Specific Weight of Fibreglass Insulation

1	2.00	5.70	1.86	21.20	22.04	3.96
2	2.00	4.20	3.62	30.41	32.31	4.04
3	2.00	7.00	1.88	26.25	25.24	3.66
4	2.00	20.00	2.56	102.40	117.12	4.36
5	2.00	1.75	1.65	7.78	5.74	3.94
6	2.00	3.62	2.22	16.07	16.26	3.84
7	2.00	6.72	2.38	31.87	32.56	3.87
8	2.00	18.38	7.00	257.32	271.64	4.02
9	2.00	18.44	7.06	256.37	282.39	4.13
10	2.00	18.44	6.28	231.61	242.55	3.99
11	2.00	6.25	2.32	29.06	35.99	4.74
12	2.00	5.76	2.44	28.11	31.05	4.21
13	2.00	13.12	1.33	34.90	32.18	3.51
14	2.00	10.31	1.36	28.04	25.74	3.51
15	2.00	19.56	1.43	55.94	61.68	4.20
16	2.00	15.03	3.69	110.92	119.18	4.10
17	2.00	5.75	2.44	28.06	30.68	4.17
18	2.00	13.31	1.81	48.18	47.87	3.78

Thermal Diffusivity of Hardboard

	Test 1		Test 2	
Time	M.V.	M.V. - $M.V._{\infty}$	M.V.	M.V. - $M.V._{\infty}$
min.				
0.00	2.359	2.053	2.360	2.056
1.00	2.037	1.731	2.043	1.739
2.00	1.448	1.142	1.456	1.152
3.00	1.044	0.738	1.046	0.742
4.00	0.783	0.477	0.782	0.478
4.50	0.689	0.383	0.687	0.383
5.00	0.615	0.309	0.612	0.308
5.25	0.583	0.277	0.578	0.274
5.50	0.551	0.245	0.551	0.247
5.75	0.529	0.223	0.523	0.219
6.00	0.507	0.201	0.503	0.199
6.25	0.482	0.176	0.481	0.177
6.25	0.465	0.159	0.463	0.159
6.75	0.447	0.141	0.442	0.138
7.00	0.434	0.128	0.433	0.129
7.25	0.417	0.111	0.418	0.114
7.50	0.409	0.102	0.405	0.101
7.75	0.398	0.092	0.394	0.090
8.00	0.389	0.083	0.386	0.082
8.25	0.378	0.072	0.378	0.074
8.50	0.373	0.067	0.369	0.065
8.75	0.364	0.058	0.362	0.058
9.00	0.360	0.054	0.356	0.052
9.25	0.353	0.047	0.352	0.048
9.50	0.348	0.042	0.347	0.043
9.75	0.344	0.038	0.341	0.037
10.00	0.341	0.035	0.338	0.034
10.25	0.336	0.030	0.334	0.030
10.50	0.334	0.028	0.331	0.027
10.75	0.329	0.023	0.329	0.025
11.00	0.328	0.022	0.327	0.023

Test 1, $M.V._{\infty} = 0.306$
Test 2, $M.V._{\infty} = 0.304$

Initial Temperatures

Node	Plane a	Plane b	Plane c	Plane d	Plane e	Plane f
1	162.3	159.2	145.8	131.5	117.1	108.2
2	162.3	159.2	145.8	131.5	117.1	108.2
3	162.3	159.2	145.8	131.5	117.1	108.2
4	162.3	159.2	145.8	131.5	117.1	108.2
5	162.3	159.2	145.8	131.5	117.1	108.2
6	162.3	159.2	145.8	131.5	117.1	108.2
7	162.3	159.2	145.5	131.0	116.9	108.0
8	162.3	159.7	145.4	131.2	116.9	108.1
9	162.3	159.8	145.7	131.2	116.8	108.2
10	162.3	159.8	145.7	131.2	116.8	108.2
11	162.3	159.2	145.8	131.5	117.1	108.2
12	162.3	159.2	145.5	130.8	116.7	107.9
13	163.2	161.5	145.3	129.3	113.2	107.8
14	163.2	161.8	145.5	129.4	113.2	107.8
15	173.2	161.8	145.5	129.4	113.2	107.8
16	162.3	159.2	145.8	131.5	117.1	108.2
17	162.3	159.2	145.5	130.6	116.3	108.0
18	162.9	160.2	145.3	129.4	113.3	107.8
19	163.2	161.8	145.3	129.2	113.0	107.8
20	163.2	161.8	145.3	129.2	113.0	107.8
21	162.3	159.2	145.8	131.5	117.1	108.2
22	162.3	159.2	145.5	130.6	116.3	108.0
23	162.9	160.2	145.3	129.4	113.3	107.8
24	163.2	161.8	145.3	129.2	113.0	107.8
25	163.2	161.8	145.3	129.2	113.0	107.8

Outside air temperature, To = 106.5

Transient Temperatures from Numerical Analysis

Time	Three Dimensional Analysis	One Dimensional Analysis
hours	T25a - To	T25a - To
0.0	55.8	55.6
0.5	49.3	48.6
1.0	43.8	43.3
1.5	39.4	38.6
2.0	35.7	34.5
2.5	32.6	30.8
3.0	29.8	27.5
3.5	27.4	24.6
4.0	25.2	22.0
4.5	23.1	19.6
5.0	21.3	17.5
5.5	19.5	15.7
6.0	17.9	14.0
6.5	16.5	12.5
7.0	15.1	11.2
7.5	13.9	10.0
8.0	12.7	8.9
8.5	11.6	8.0
9.0	10.6	7.1
9.5	9.8	6.3
10.0	9.0	5.7
10.5	8.3	5.1
11.0	7.6	4.5
11.5	7.0	4.0
12.0	6.4	3.6
12.5	5.9	3.2
13.0	5.4	2.9
13.5	5.0	2.6
14.0	4.6	2.3
14.5	4.2	2.1
15.0	3.9	1.8
15.5	3.5	1.6
16.0	3.2	1.5
16.5	3.0	1.3
17.0	2.7	1.2
17.5	2.5	1.0
18.0	2.3	0.9
18.5	2.1	0.8
19.0	1.9	0.7
19.5	1.8	0.7
20.0	1.6	0.6

Time	Three Dimensional Analysis	One Dimensional Analysis
hours	T25a - To	T25a - To
20.5	1.5	0.5
21.0	1.4	0.5
21.5	1.3	0.4
22.0	1.2	0.4
22.5	1.1	0.3
23.0	1.0	0.3
23.5	0.9	0.3
24.0	0.8	0.2

Transient Temperatures from Experiment

Time	Test 1	Test 2
hours	T25a - To	T25a - To
0.0	57.1	56.6
1.0	49.3	49.6
2.0	43.6	43.1
3.0	37.1	36.9
4.0	30.9	30.7
5.0	27.1	26.2
6.0	23.1	22.6
7.0	19.6	19.9
8.0	16.9	18.0
9.0	13.5	16.0
10.0	10.9	13.7
11.0	9.3	9.7
12.0	7.8	6.9
13.0	6.1	5.7
14.0	4.9	4.8
15.0	4.0	3.9
16.0	3.3	2.9
17.0	2.6	1.9
18.0	1.8	0.9

To correct for error in recorder timing system, multiply times by 0.96

APPENDIX G. FIGURES

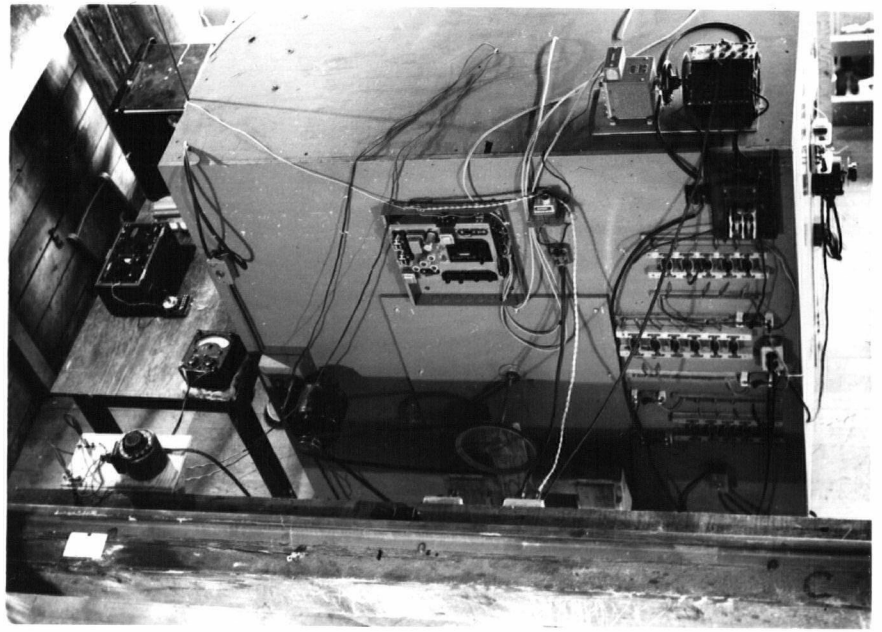

FIG. 1 GENERAL VIEW OF APPARATUS

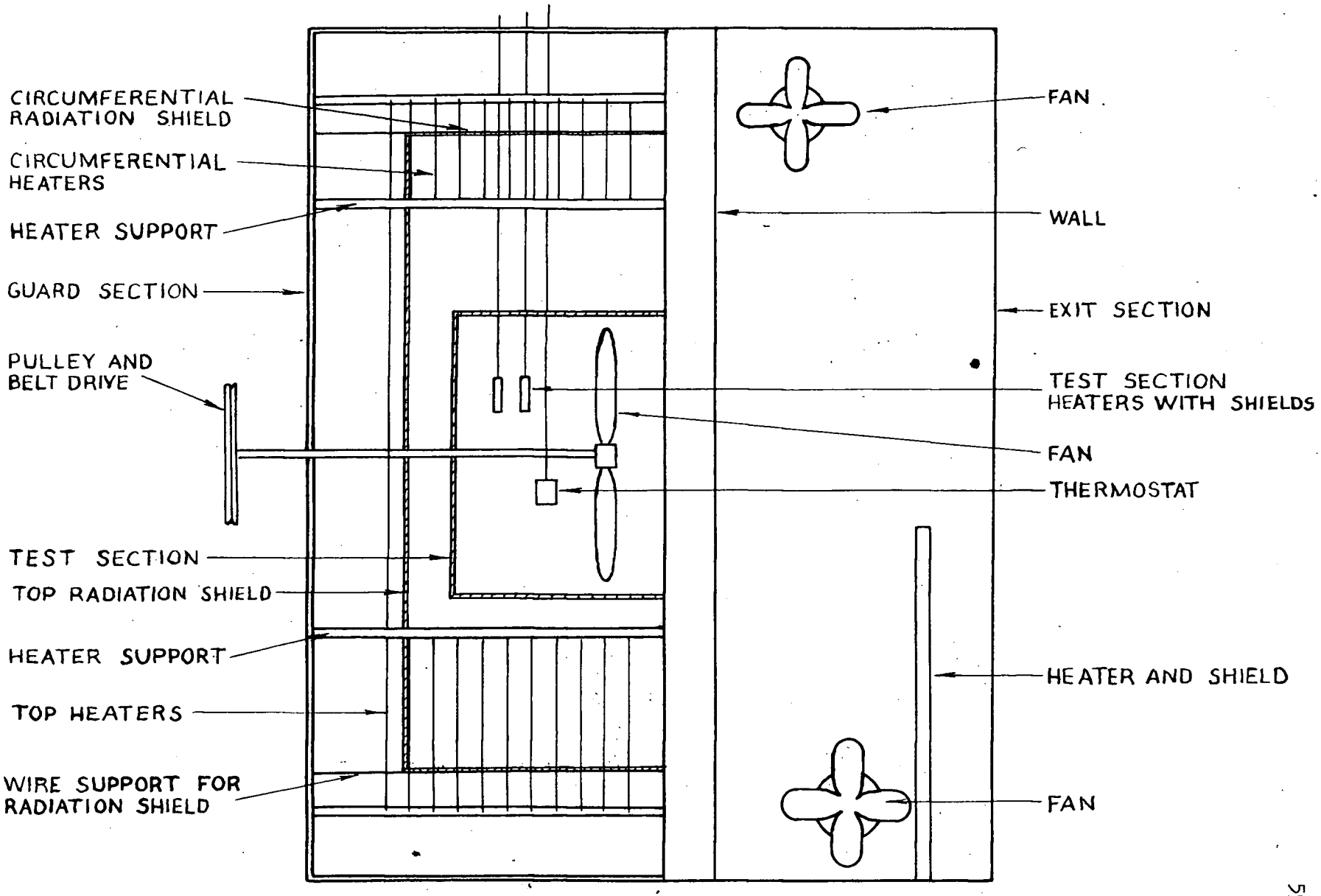

FIG. 2 SIDE SECTION OF APPARATUS

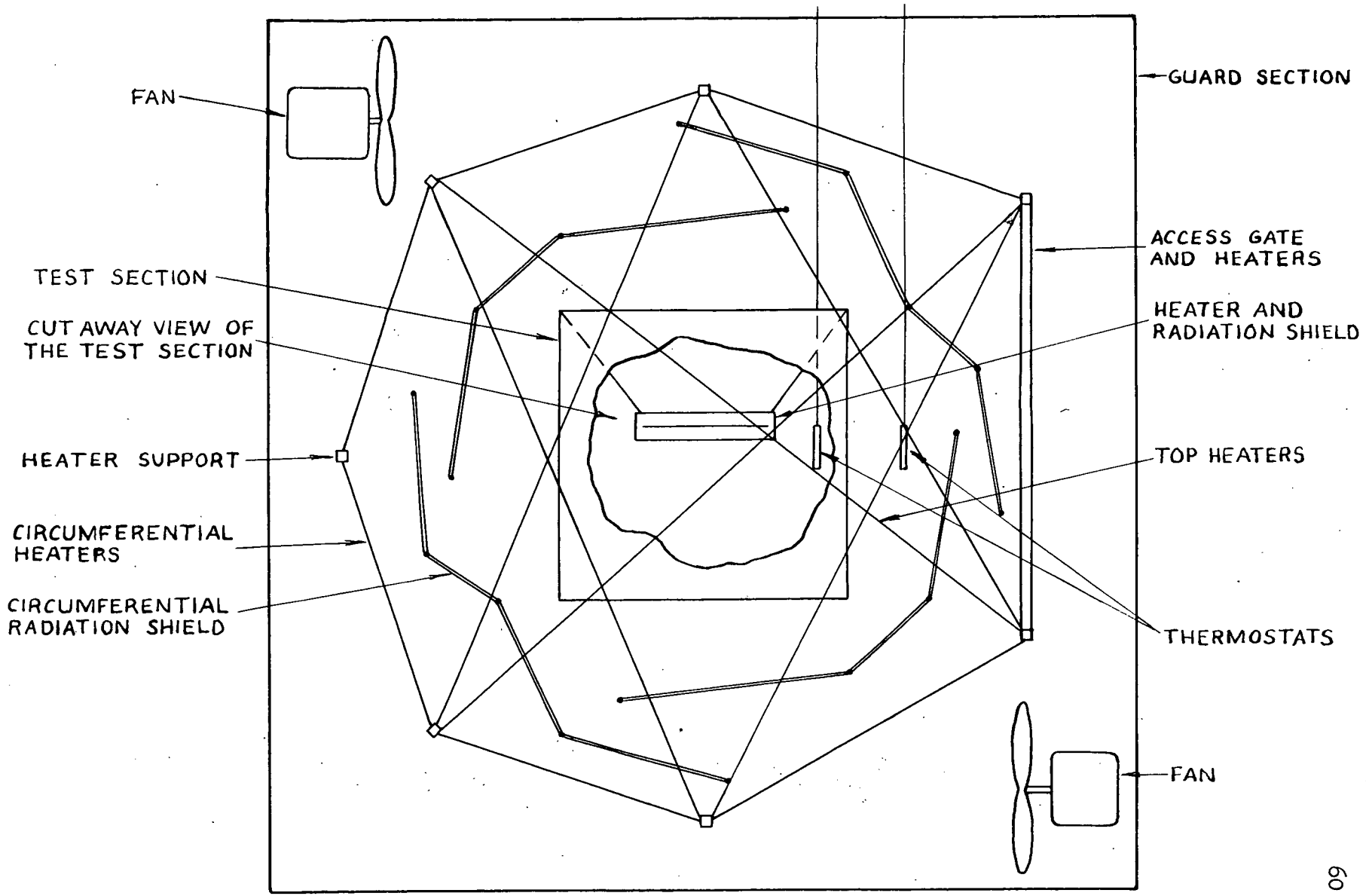

FIG.3 FRONT SECTION OF THE APPARATUS

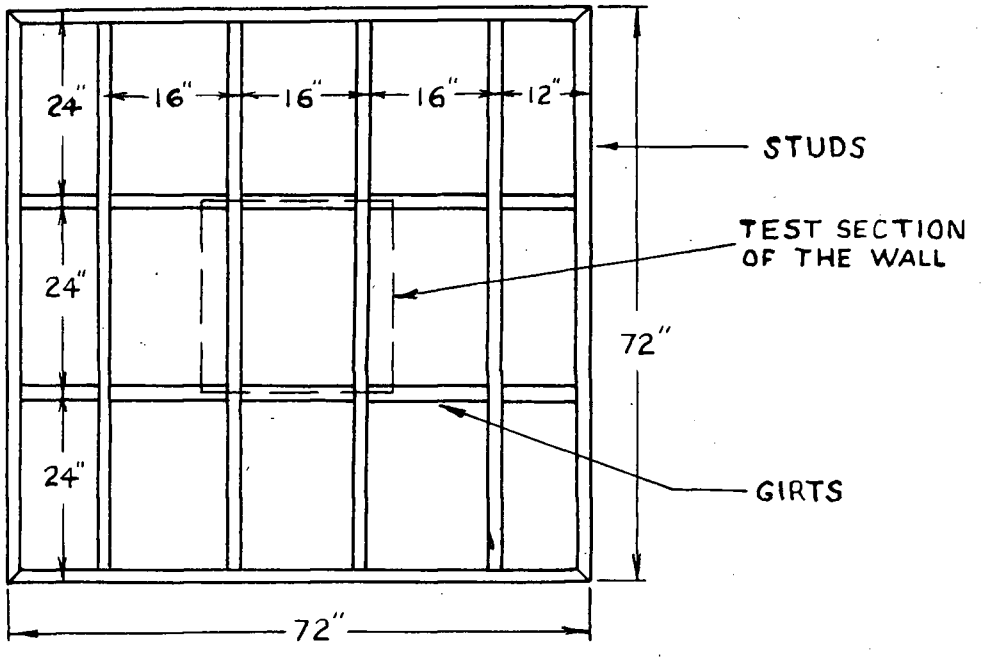

FIG. 4 FIR FRAME

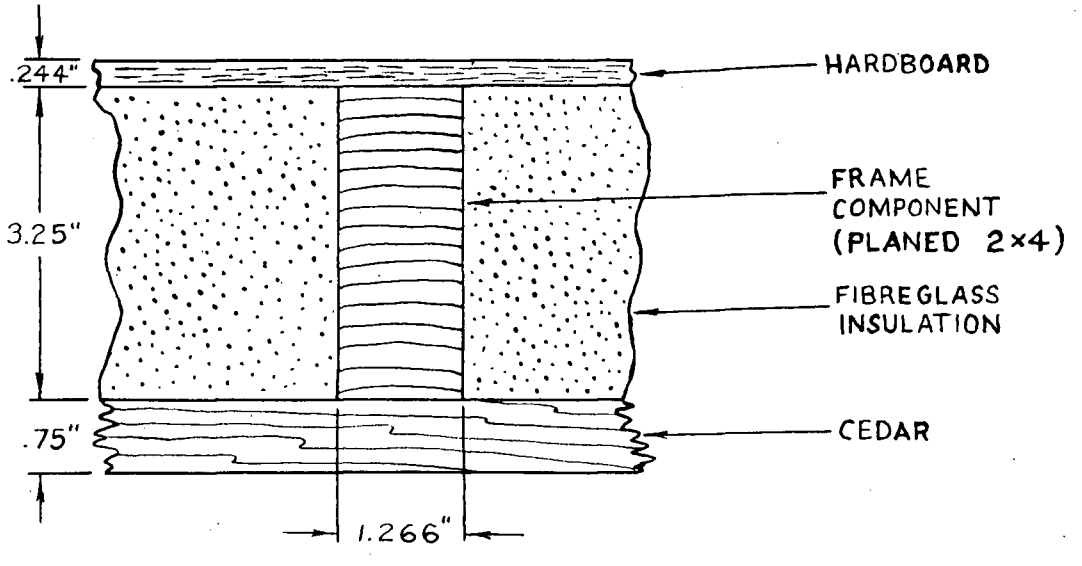

FIG. 5 CROSS SECTION AT A FRAME COMPONENT

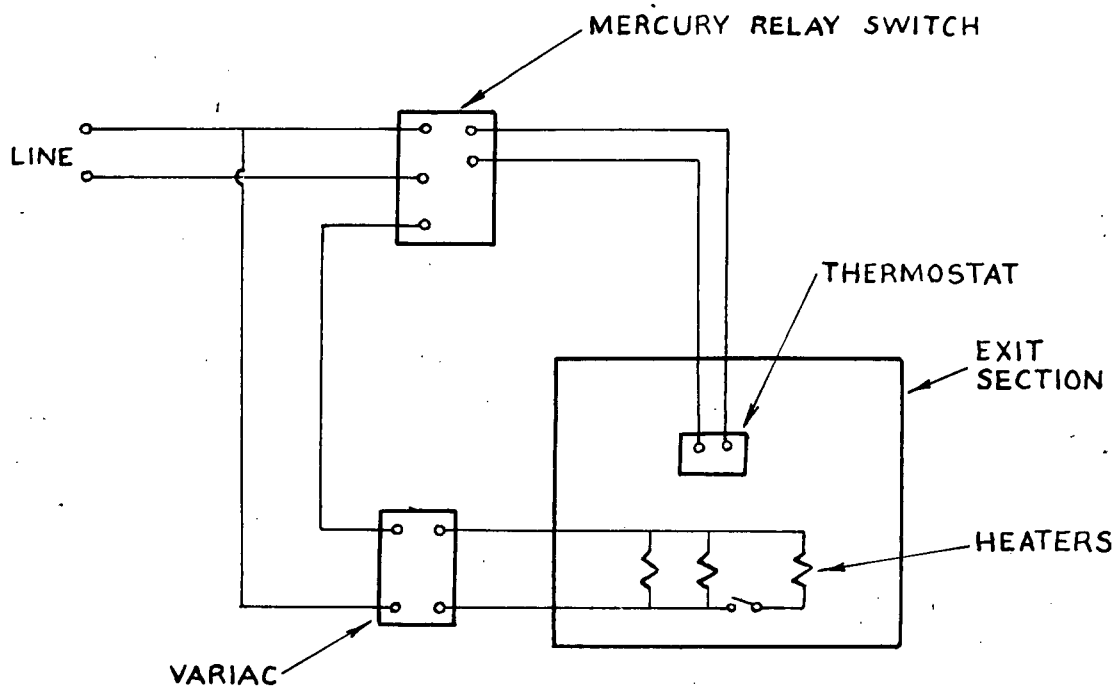

FIG. 6 TEMPERATURE CONTROL SYSTEM FOR THE EXIT SECTION

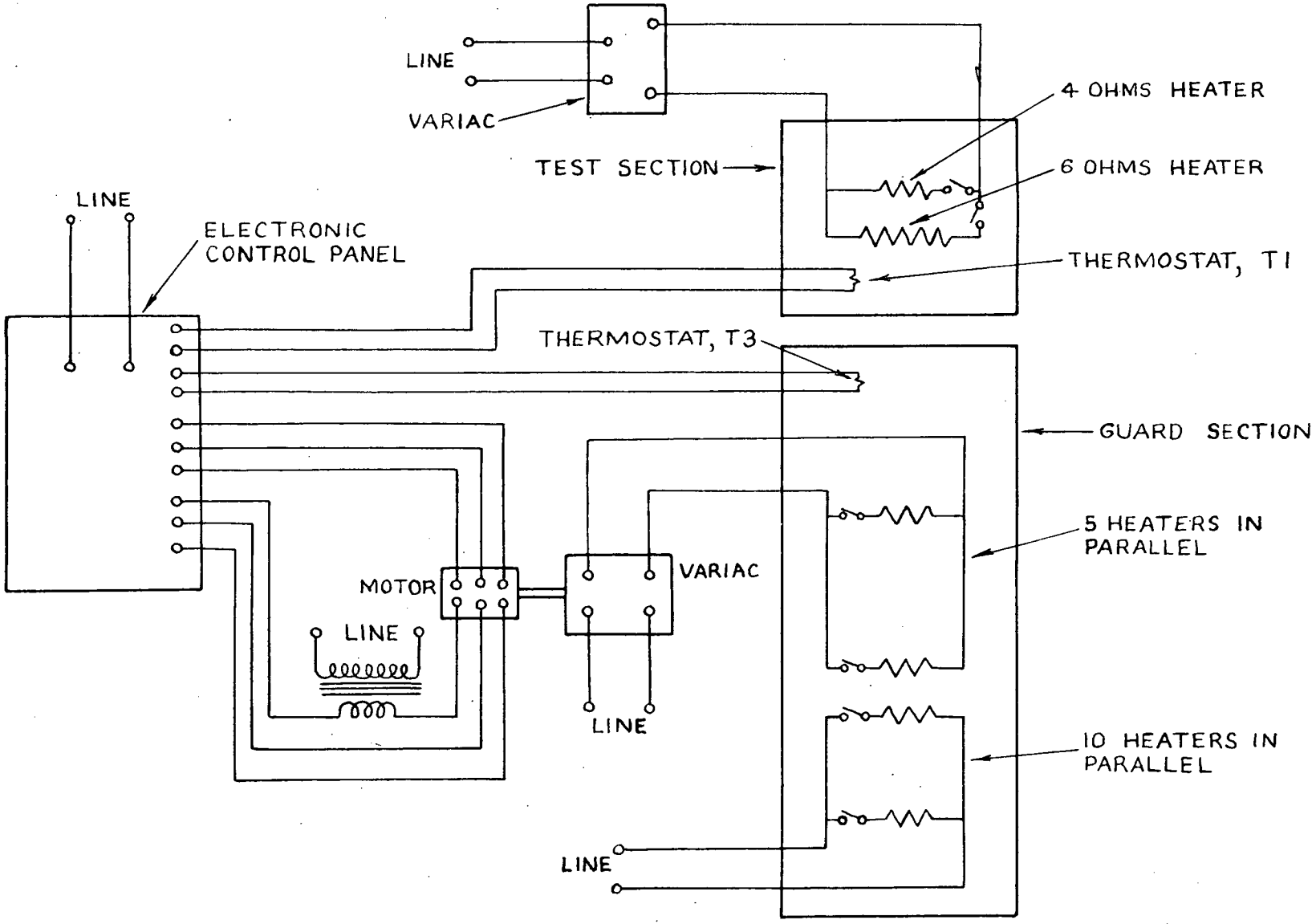

FIG. 7 HEATER AND CONTROL CIRCUITS FOR THE TEST AND GUARD SECTIONS

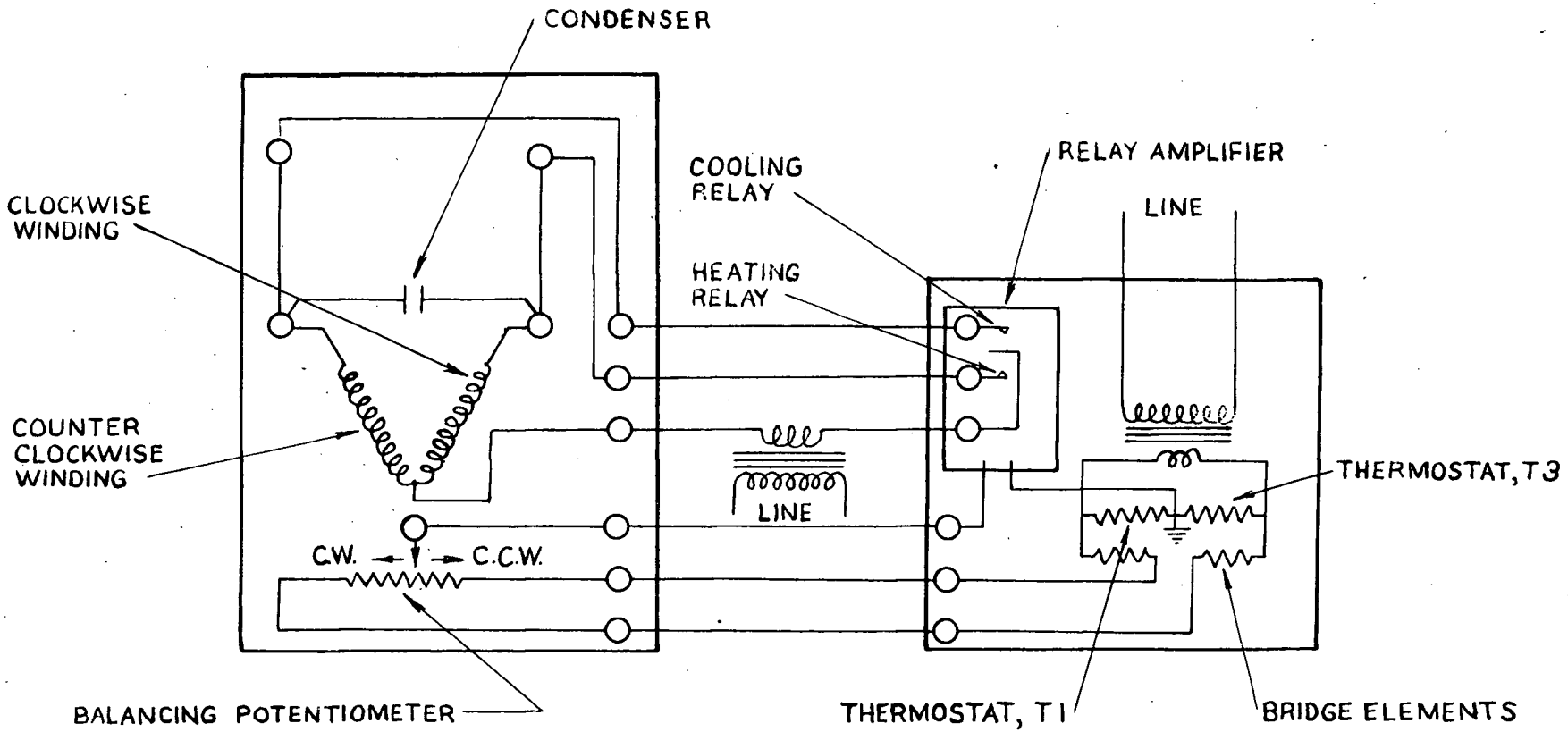

FIG. 8 SIMPLIFIED ELECTRONIC CONTROL CIRCUIT

FIG. 9 RECORDER AND THERMOCOUPLE SWITCH BOX

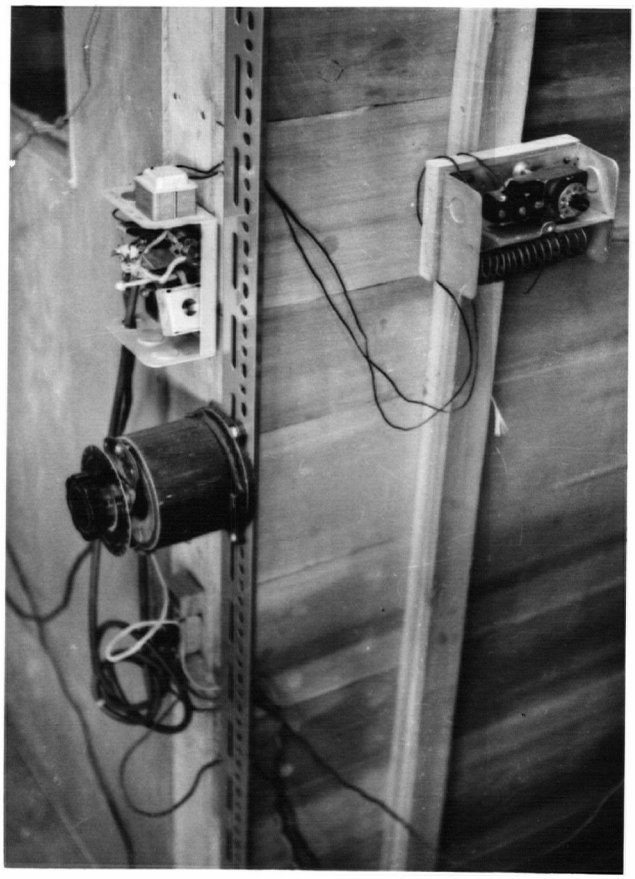

FIG. 10 WALL AND COMPONENTS OF EXIT SECTION TEMPERATURE CONTROL SYSTEM

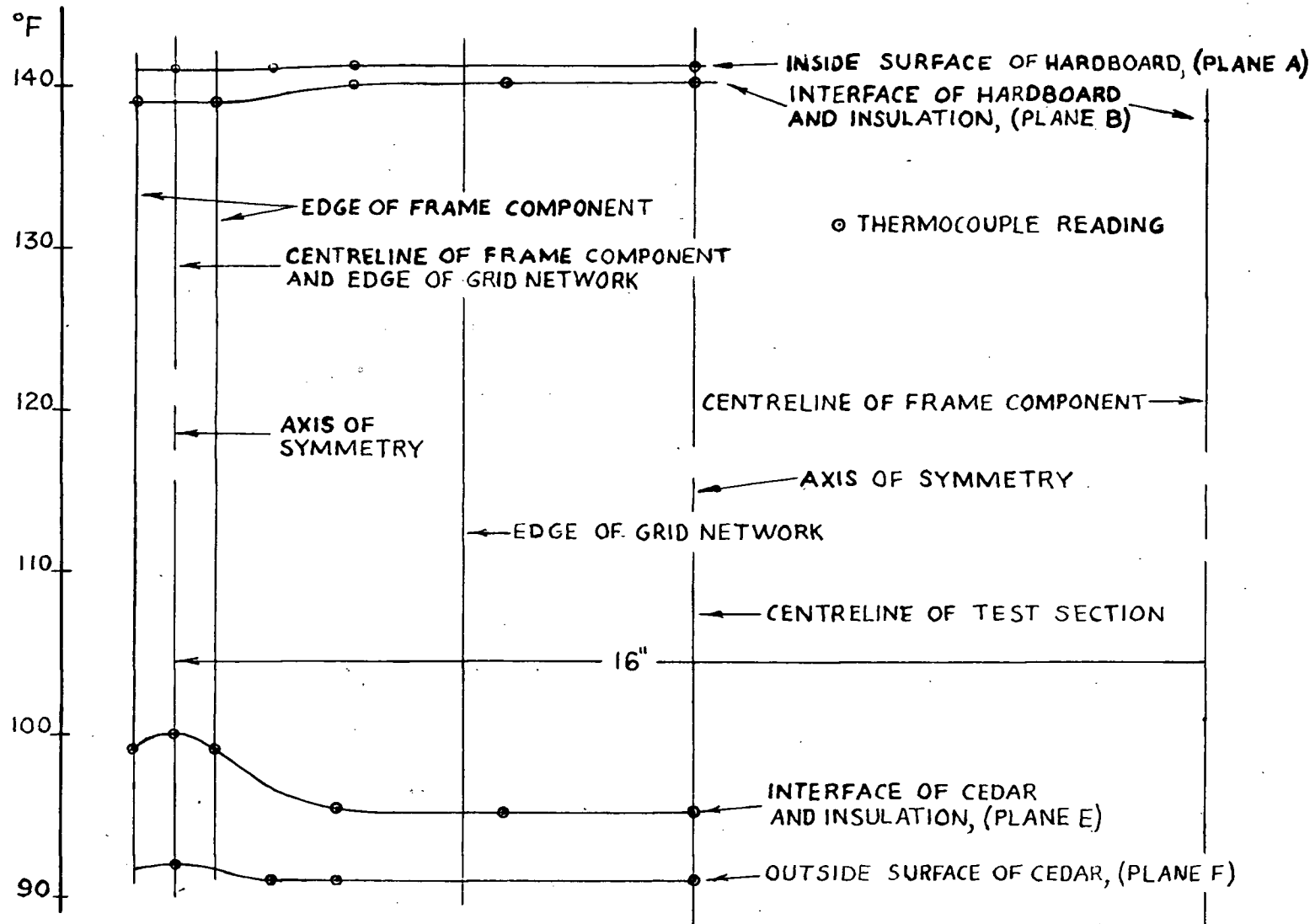

FIG. 11 STEADY STATE TEMPERATURES

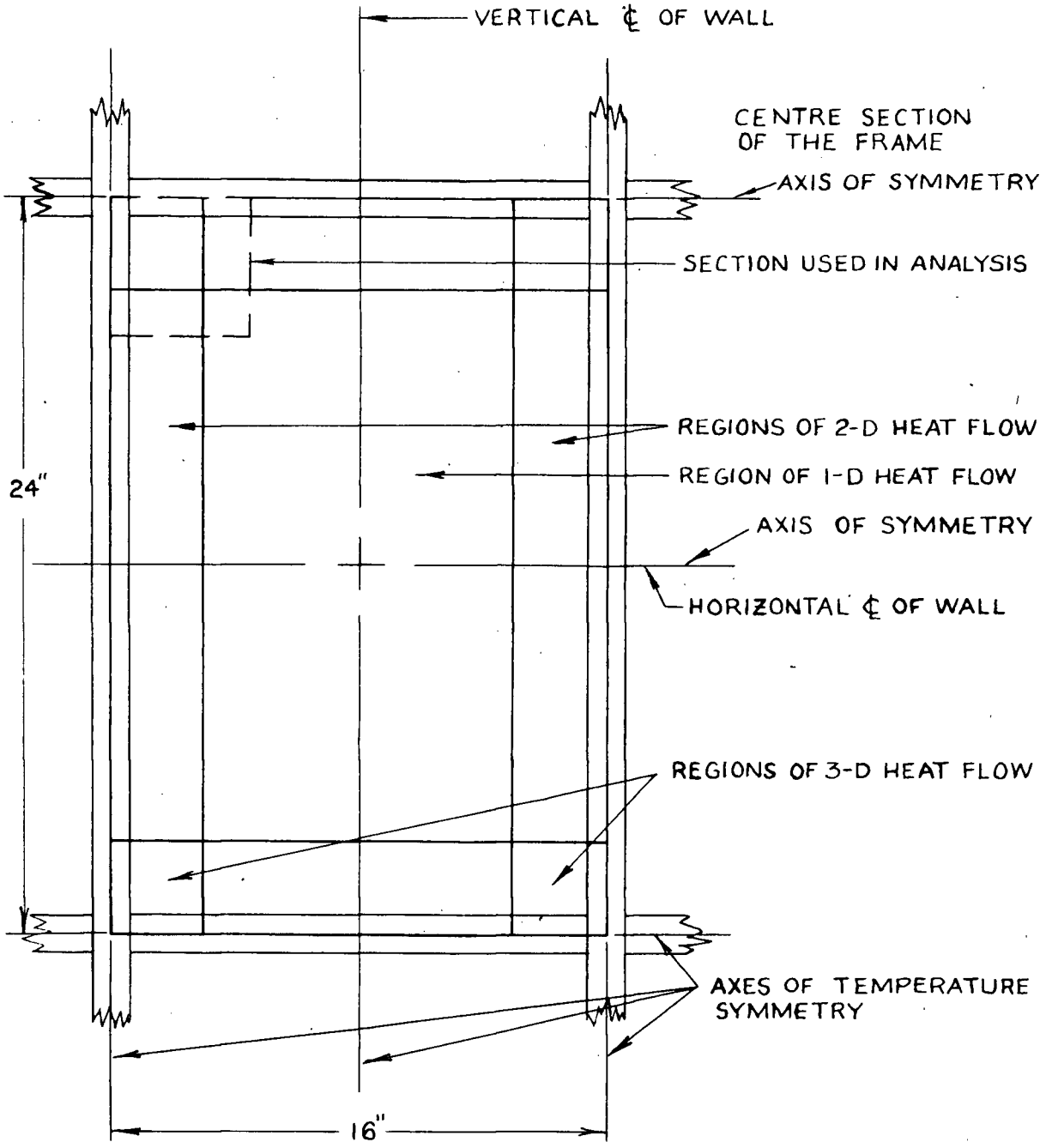

FIG. 12 AXES OF TEMPERATURE SYMMETRY AND REGIONS OF HEAT FLOW

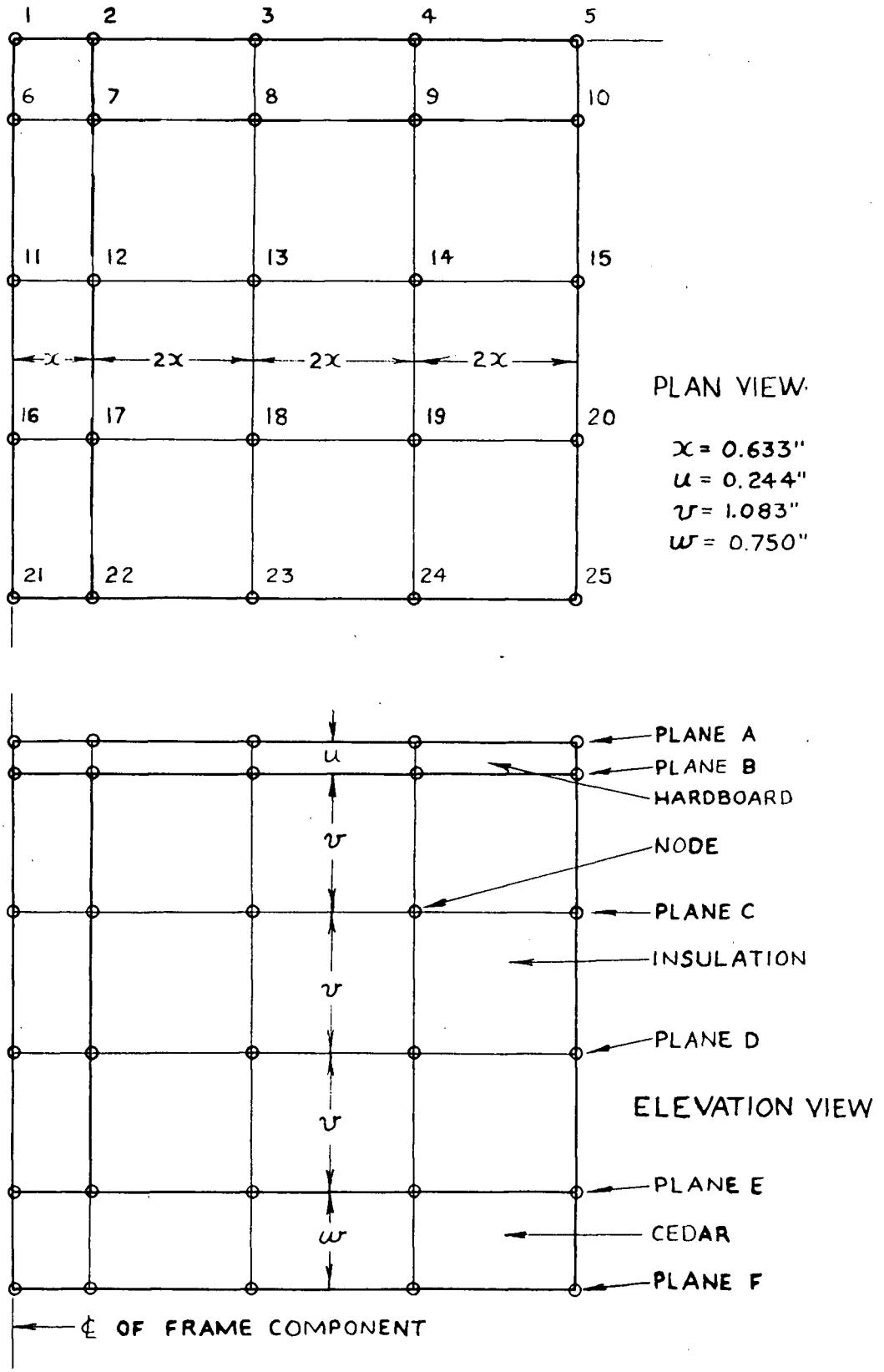

FIG.13 NODE SYSTEM FOR ANALYSIS

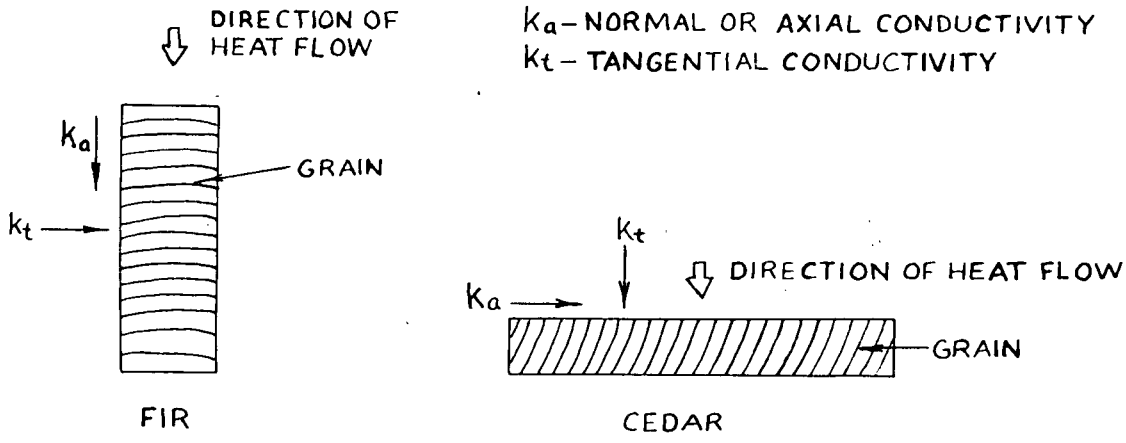

FIG.14 AXIAL AND TANGENTIAL CONDUCTIVITIES

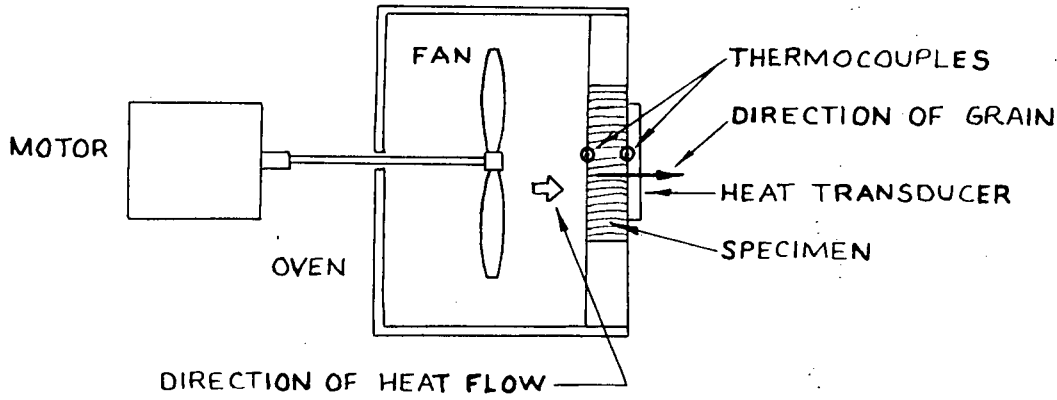

FIG.15 APPARATUS FOR LONGITUDINAL CONDUCTIVITY TESTS

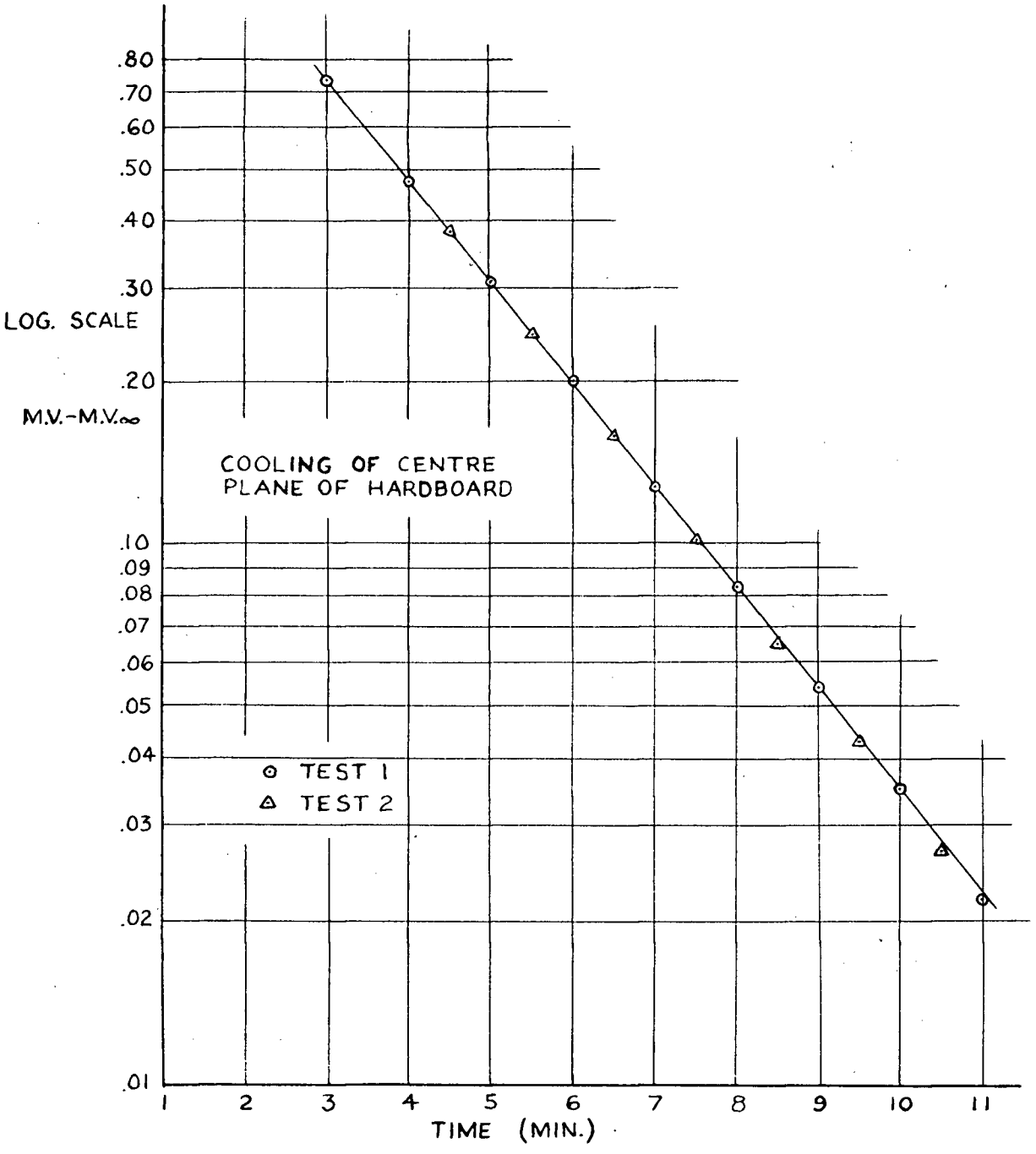

FIG. 16 THERMAL DIFFUSIVITY TESTS FOR HARDBOARD

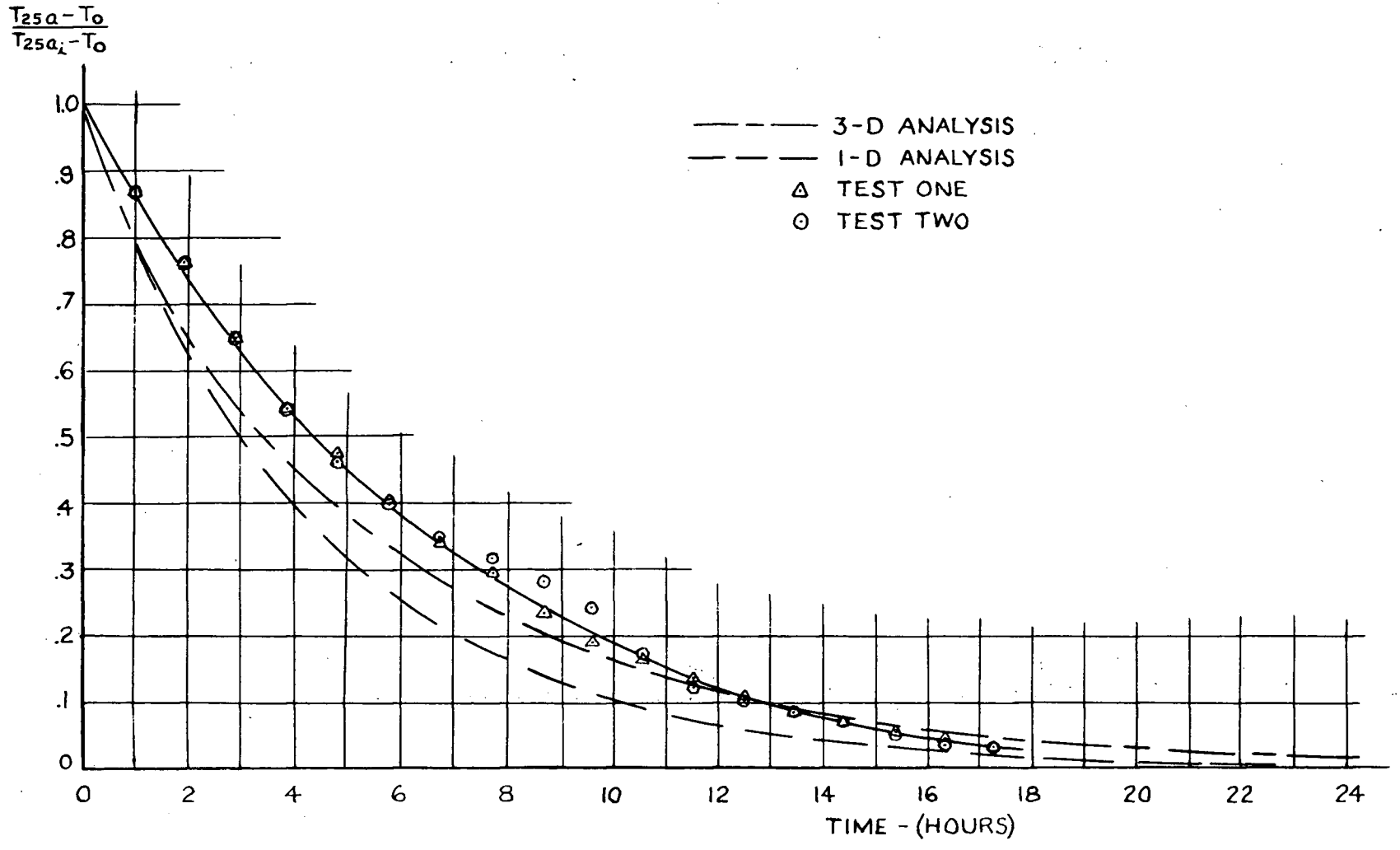

FIG. 17 COOLING CURVES FOR INSIDE WALL SURFACE

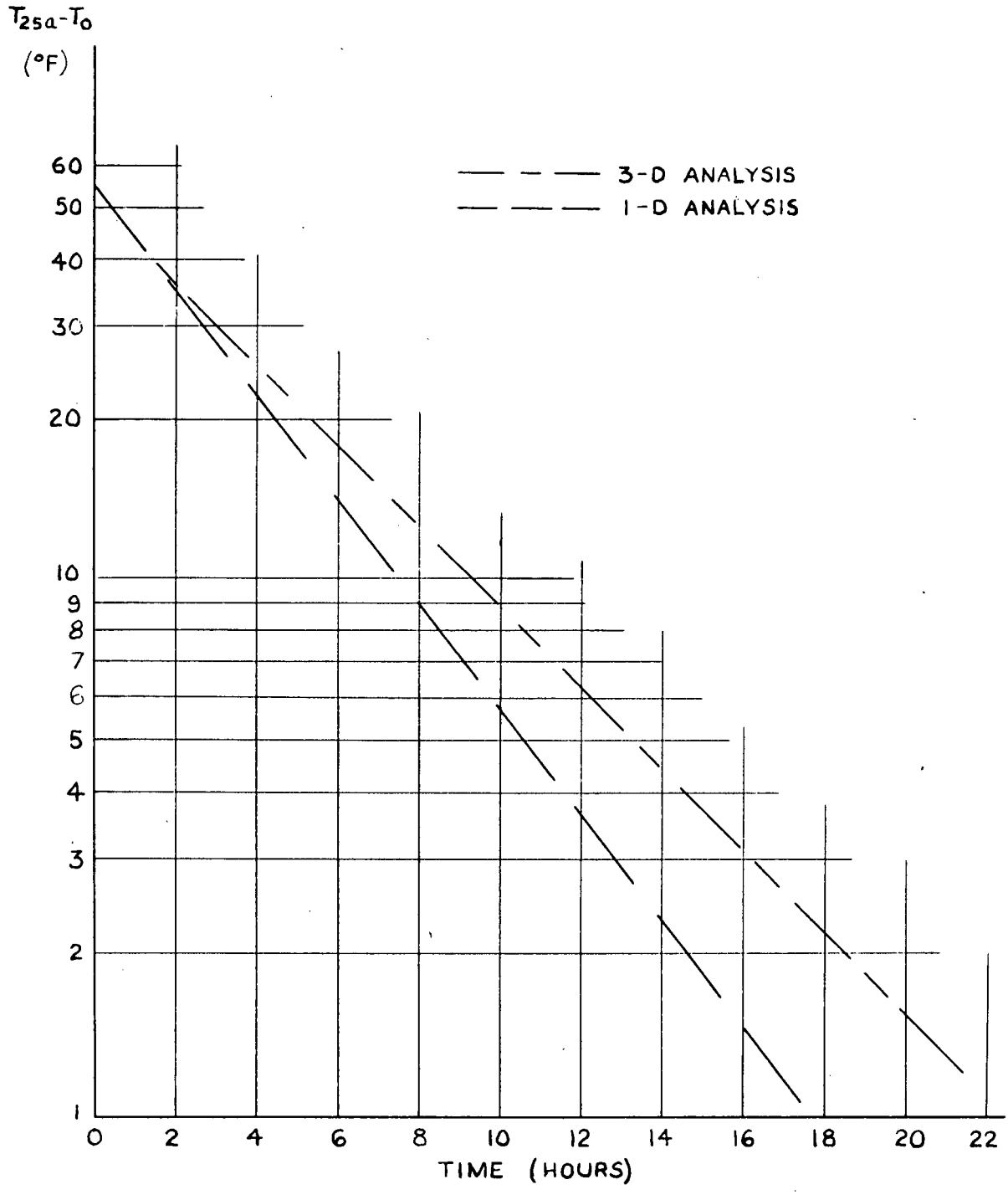

FIG. 18 THEORETICAL COOLING CURVES

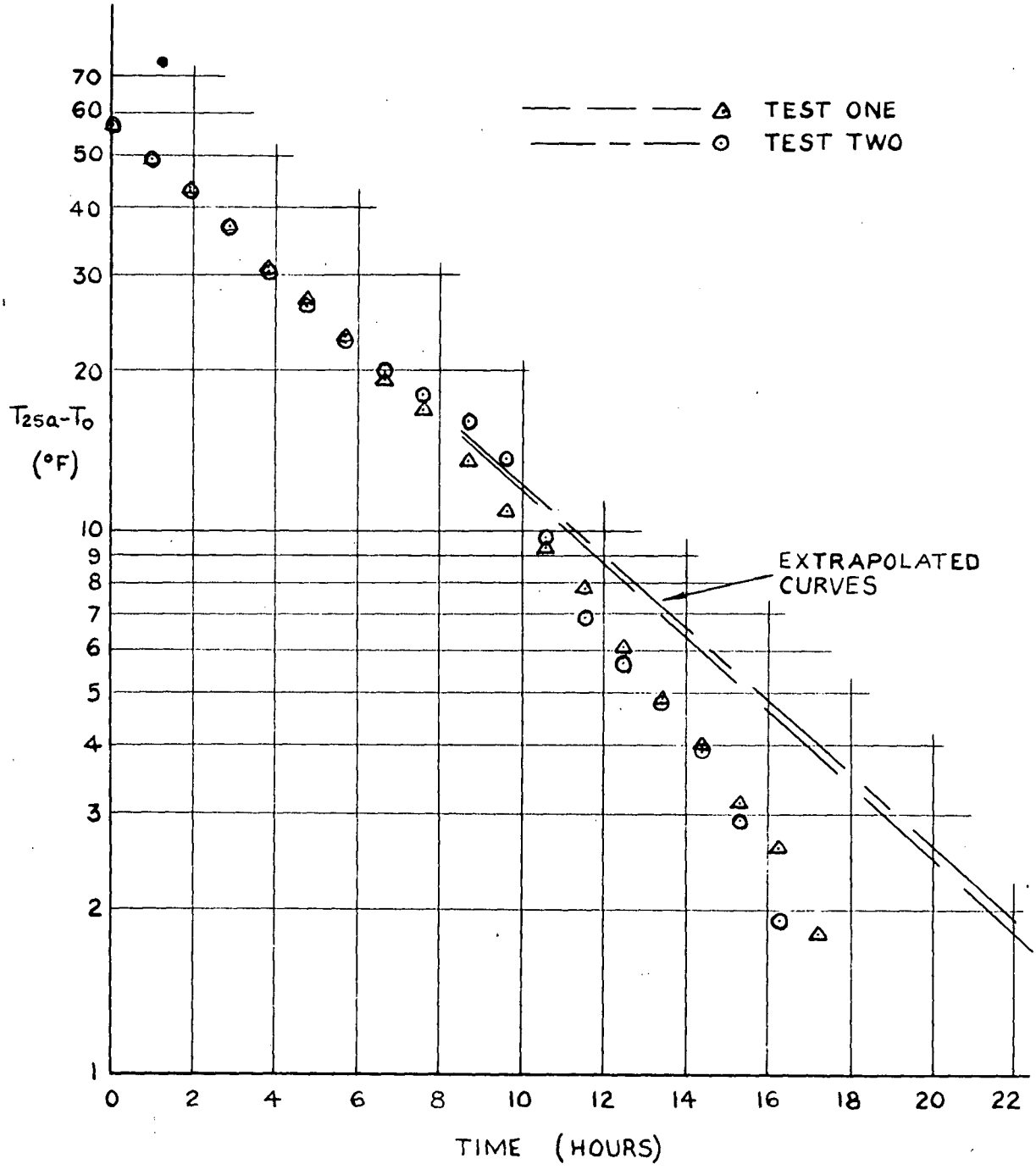

FIG. 19 EXPERIMENTAL COOLING CURVES

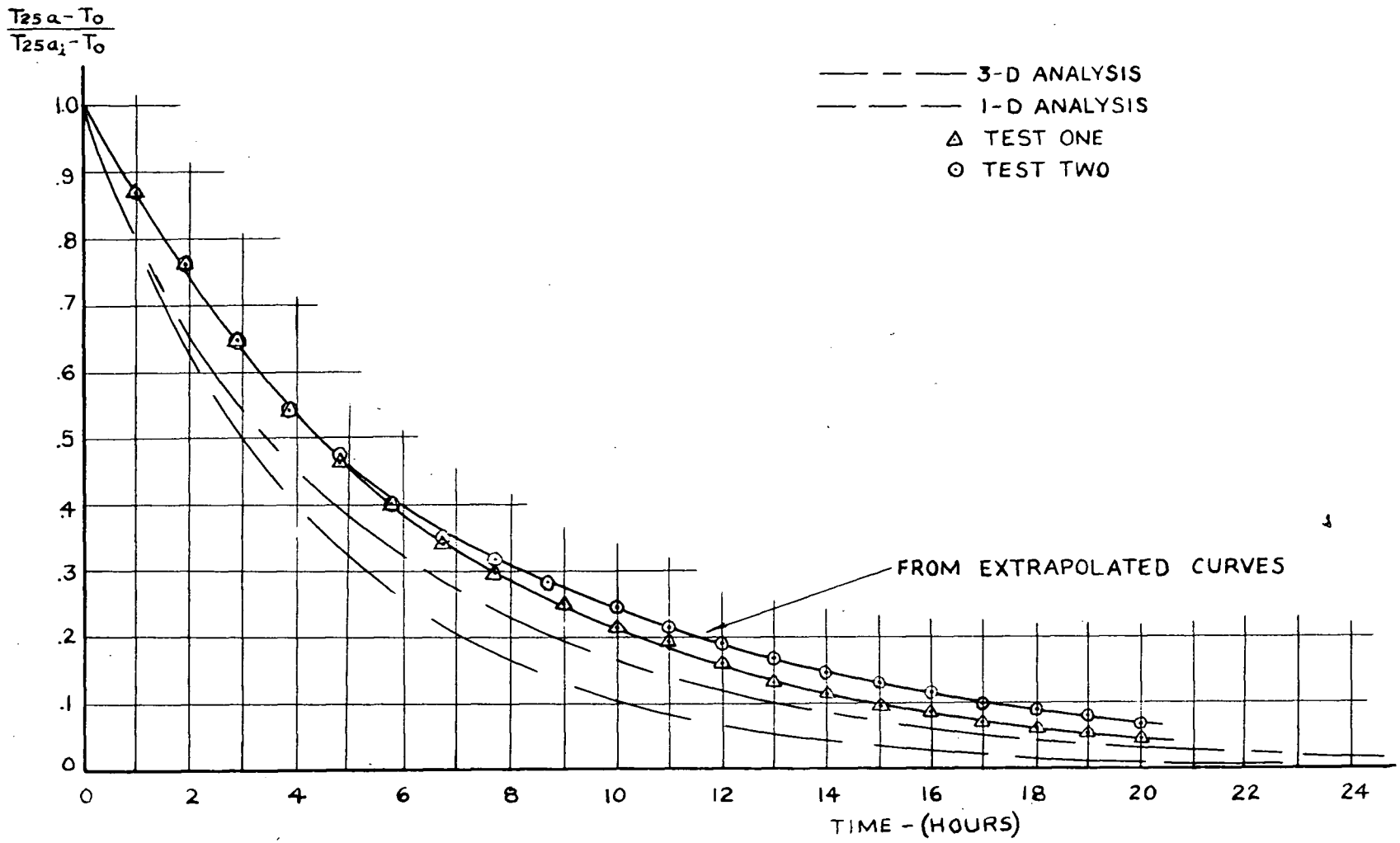

FIG. 20 THEORETICAL AND CORRECTED EXPERIMENTAL COOLING CURVES